

2021

Analysing and improving the structural stiffness of the Triumph Vitesse

Jones, Chris

Jones, C. (2021) 'Analysing and improving the structural stiffness of the Triumph Vitesse', The Plymouth Student Scientist, 14(1), pp. 246-285.

<http://hdl.handle.net/10026.1/17331>

The Plymouth Student Scientist
University of Plymouth

All content in PEARL is protected by copyright law. Author manuscripts are made available in accordance with publisher policies. Please cite only the published version using the details provided on the item record or document. In the absence of an open licence (e.g. Creative Commons), permissions for further reuse of content should be sought from the publisher or author.

Analysing and improving the structural stiffness of the Triumph Vitesse

Chris Jones

Project Advisor: [Adam Kyte](#), School of Engineering, Computing & Mathematics, University of Plymouth, Drake Circus, Plymouth, PL4 8AA

Abstract

The Triumph Vitesse is a British sports car built by British Leyland in the 1960s as a development from the Herald and sharing common design features with the Spitfire and GT6. Vehicle stiffness has a direct impact on handling, passenger comfort and safety, and so modern manufacturers invest time and money in enhancing structural properties of their products.

This research aimed to quantitatively analyse the structural stiffness of the Triumph Vitesse and identify weak areas suitable for targeted improved. This was achieved by modelling the vehicle structure in Solidworks and conducting a Finite Element Analysis (FEA). A test rig was constructed and the torsional stiffness of the Vitesse established experimentally. The FEA results were then validated against the experimental data, and the verified virtual models used to develop modifications that enhance vehicle stiffness. The research was successful; the chassis was found to have stiffness of 1250Nm/deg with the body structure increasing stiffness by 90%, and the doors and convertible roof adding a further 20% each to reach an overall stiffness of 3500Nm/deg. Tested chassis modifications increased chassis stiffness by 37%, and virtual tests suggest that the fitment of an additional sill structure could increase overall stiffness by 35% to 5400Nm/deg. This would make the Vitesse comparable with the BMW Z3 and Mazda MX5 with 5600Nm/deg and 6000Nm/deg respectively.

Keywords: Triumph Vitesse, British Leyland, structural stiffness, vehicle stiffness, chassis stiffness, modifications, handling, Finite Element Analysis.

Introduction

The Vitesse is a small chassis Triumph, manufactured in the 1960s, based on the Herald and sharing common design features with the Spitfire and GT6. These models are known as the 'Small Chassis' Triumphs due to their separate backbone chassis, 'flip front' bonnets and bolt on bodies. The backbone chassis was a controversial choice at the time as separate chassis were becoming obsolete in favour of stronger and stiffer 'monocoque' structures (Thomason, 2003). This arrangement the cost effective production of parallel models and produced a "light and rigid structure" (Standard Triumph, 1962, pp.4). However, since the chassis must be accommodated under the floor the sectional height is low reducing structural strength, and the added stiffening effect of the body tub is limited by the body mount interface.

This study will combine physical testing and FEA methods to quantify how stiff the Triumph Vitesse is, and assess the contribution of chassis, engine and body structure to overall stiffness. This assessment will then be used to identify the weakest areas and direct improvement strategies. Design concepts will be developed and tested against the baseline results. Modifications are focussed on road use rather than track, so solutions must comply with UK road regulations and not detract from the vehicles' practicality.

Vehicle stiffness has a direct effect on handling and passenger security, as well as overall crashworthiness and safety. Whilst project findings and recommendations cannot be used by Triumph, the methods and tools used are directly applicable to a wide range of engineering problems (Karayan *et al*, 2012). The results may also be useful to enthusiasts wishing to improve vehicle performance and safety.

Literature Review

The original Herald Mk1 chassis was tested before production as described in "Turn left for Tangier – the hard way for Heralds", after which a number of structural updates were incorporated (Bensted-Smith, 1960). Despite this, the Indian export model, the Standard Gazel, evolved rapidly, dropping the flip front in favour of fixed front wings and re-engineering the rear chassis and suspension (Bhote, 2005). When the Vitesse was introduced, it boasted a "completely redesigned chassis" with deeper box sections and "internal sleeves" (Autocar, 1962, pp.6). In 1991 Pettifor proved experimentally that the broadly similar Triumph Spitfire chassis has a stiffness of 1225 Nm/deg.

However, anecdotal evidence confirms that both Vitesse and Herald flex noticeably when jacked up or parked on uneven surfaces, to the extent that the doors no longer open and panel gaps are meaningless (Club Triumph Forum, 2015; Sideways Forum, 2019).

Low torsional stiffness also has a detrimental effect on the handling characteristics; see Appendix A for analysis. Modern designers focus on torsional stiffness since this is hardest to improve – structures with good torsional stiffness typically have good bending stiffness (Robertson, 2002).

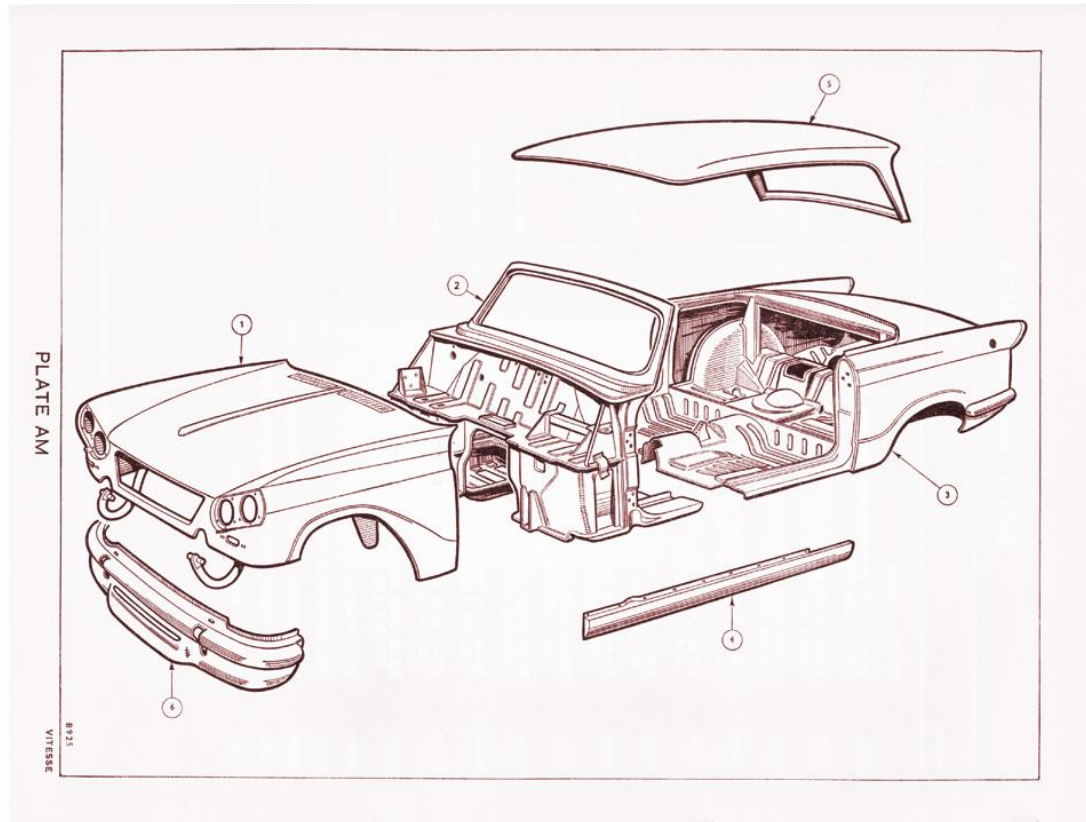


Figure 1: Triumph Vitesse body sub-assemblies, reproduced by kind permission of Canley Classics.

The main body structure (fig.1: Canley Classics, 2020) is in two halves (2 & 3) and the roof (5) is a bolt on addition, fitted over a rubber seal. The bonnet (1) flips forward and the sill panels (4) are purely cosmetic, fitted with self tapping screws. (Standard Triumph, 1962) There is no significant attempt to strengthen the structure between the convertible and saloon variants.

Convertible models must be strengthened in sills, and cross-members added to reinforce the diagonals that would have been braced by the roof structure. Despite this, even modern convertibles are significantly weaker than saloon models. For example the Porsche 911 Turbo 996 has a torsional stiffness of 27,000 Nm/deg whilst the convertible variant has a stiffness of 11,600Nm/deg, a decrease of 60% despite being 70kg heavier (Parkers, No Date). Similarly the 2003 ford mustang convertible is 70% less stiff and 60kg heavier (YouWheel, 2016).

This is expected since the roof structure contributes additional cross sectional area at a distance from the structures neutral axis. The distance is significant since the parallel axis theorem relates the second moment of area (I_z) to the distance (r) squared:

$$I_z = I_x + Ar^2 \quad (\text{Shigley, 2015})$$

Generally, the larger the structure's I_z , the greater the resistance to deformation (Shigley, 2015).

The UK DVLA does not list a required torsional stiffness or acceptable test method, however the Australian government specify a standard test procedure for modified and specialist vehicles – MR810 (Government of South Australia, 2019). In this test ‘all hinged panels’ are opened and the vehicle loaded with a torque 25% of the gross vehicle mass multiplied by the vehicle track or width. This may not be helpful since this test is for relative stiffness against an unmodified vehicle.

Pettifor (1991) attempted to enhance the stiffness of a Triumph Spitfire for race use, analysing chassis stiffness through computer FEA and mechanical testing. Since the Spitfire and Vitesse share a similar structure and layout, as can be seen in Figure 2 (Canley Classics, 2020), the methods and reasoning applied may be compared directly.

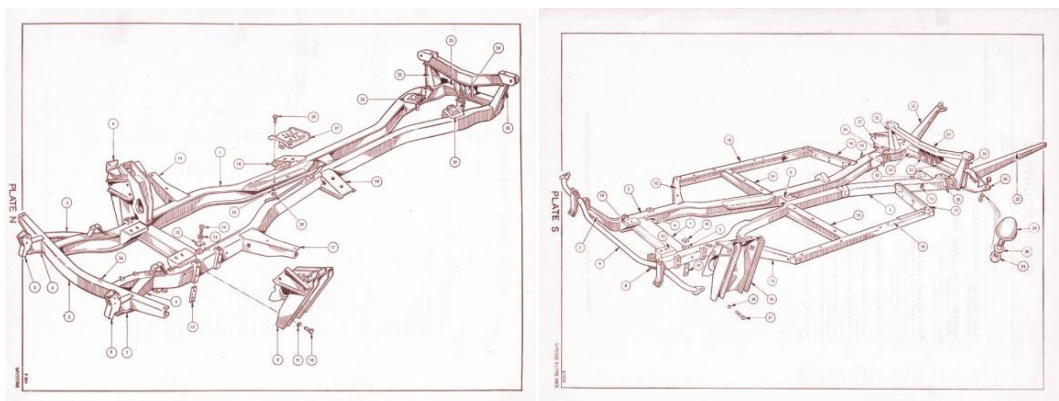


Figure 2: Triumph Spitfire and Vitesse chassis comparison, reproduced by kind permission of Canley Classics

Through experimentation, chassis stiffness was found to be 1225Nm/degree – within 2.6% of a previous 1988 study of the same model by engineers of the Raynard Racing team. The FESDEC FEA software was used to simulate the experiment, yielding a result within 5% of experimental values. Therefore, this result is considered acceptably accurate and will be used as a benchmark for setting up models in this study.

Pettifor’s modifications to improve stiffness included a welded cross-member ahead of the diff reminiscent of the ‘T-Shirt plate’ used on the Triumph TR series vehicles (Sideways Forum, 2019). This increased stiffness by 20%, and a bolt on cage structure on one side of the vehicle which increased stiffness by 62%, though it displaced the passenger seat.

Pettifor focuses on the chassis structure, since “the main strength of the structure is the chassis” (Standard Triumph, 1962, pp.5). However the bolt on body assemblies must increase structural stiffness since I_z is increased, these effects should be quantified and improvements considered.

Computer Analysis

FEA Theory

Throughout this project, Solidworks 2017 was used for both modelling and simulation. The simulations undertaken are finite element analysis (FEA), this technique uses the finite element method (FEM) to divide a complex problem into millions of elements, this is known as meshing. Calculations are performed on each element and assembled as a colour plot of the specified parameter for user analysis (Solidworks, 2017). The model boundaries must be setup and meshed appropriately, and the correct solver applied to produce an accurate representation of reality. Despite this, it is a useful tool and can reduce the time and expense of building and testing multiple prototypes. To ensure the correct solution is reached quickly, simple validation cases with known solutions are used to build up to the full problem.

Validation Cases

Simple solid, open (C) and closed (box) beam sections (Figure 3) were considered initially. Stress and deflection were calculated in bending and torsion. These cases were then modelled in FEA and the results validated against the calculated values.



Figure 3: Simple beam sections considered (Solid, Open and Closed)

Hand Calculations

The bending beam theory and calculations used were taken from Hibbeler (2011) and Torsion cases from Roark (2002) and Shigley (2015); calculations and formulae may be seen at Appendix 1.

Equation 1 was used to calculate the angle of twist and is the foundation of the calculations used later in the report.

$$\theta = \frac{TL}{kG} \quad [1] \text{ (Shigley, 2015)}$$

It is a critical assumption in the torsion calculations that the ends are free to move out of plane or 'warp', unlike circular section beams. The open section calculations are based on the membrane analogy – the cross section of the 'flattened' net responds in the same way as the formed shape. The dimensions used are approximately those of the chassis main rails to be sure of an appropriate scale for comparison.

FEA Setup and Test

All simulations in this project use the material properties of AISI 1020 steel from the Solidworks 2017 materials library (Table 1). This is a good generic structural steel and the properties are the same as those used in Pettifor's 1991 study. Unless otherwise stated, the linear-static study is used, since metals obey Hookes law until they yield.

Table 1: Material Properties of AISI 1020 Steel as used in Solidworks 2017

Property	Value	Unit
Elastic Modulus	205	GPa
Poisson's Ratio	0.29	-
Shear Modulus	80	GPa
Mass Density	7870	kgm ⁻³
Tensile Strength	420	MPa
Yield Strength	350	MPa

* Solidworks 2017 Material Library

The bending cases were fixed at one end in all DOF, and the other allowed to move axially. Load was applied to a central split-line as in Figure 4.

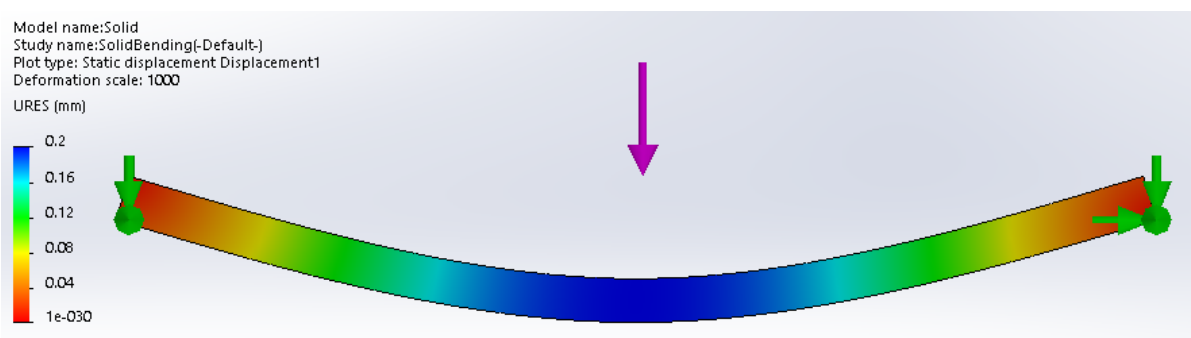


Figure 4: Resultant Displacement Plot of Bending Beam Simulation at 1000N

In the pure torsion case, the fixtures must allow warping whilst fixing the component in space. In addition, since there is axial stress and strain, the component may lengthen under twist as shown by Poynting (1909). Therefore the fixtures used must also allow axial translation whilst fixing one node in all DOF, as in Figure 5.

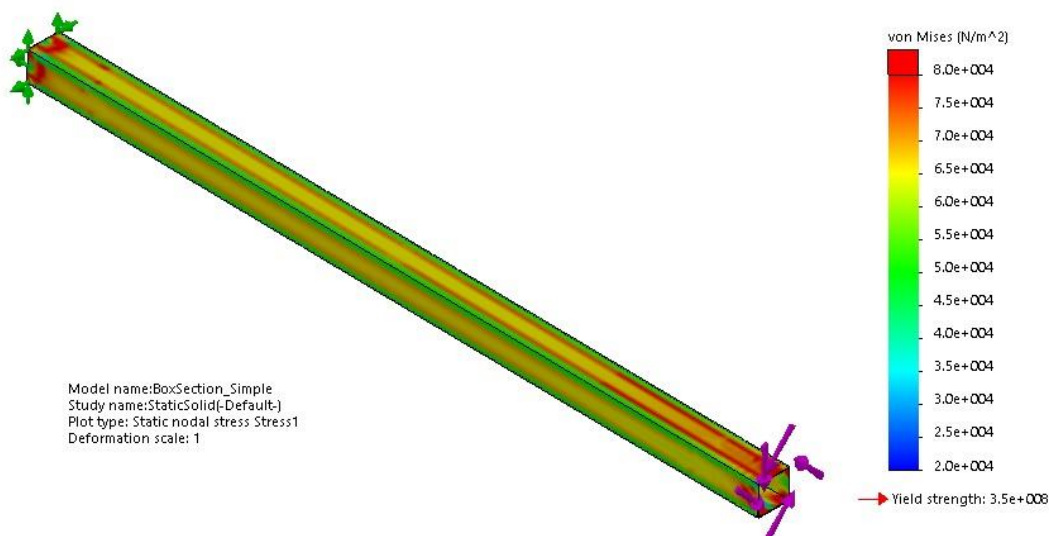


Figure 5: Closed Section Beam Simulation - Torsion Case

Mesh Independence

The mesh used to simulate the model influences the quality of results. The ideal mesh is a compromise between solution accuracy - finer mesh for a better resolution - and fast solve time - fewer elements, fewer equations to solve (Solidworks, 2017). To assess mesh independence, simulations were rerun initially with a much finer, then a much coarser mesh, as in figure 6. Deflection and stress were plotted against the number of mesh elements to establish if they were influenced by the mesh changes. The below Graphs, 1 and 2, show that both parameters are stable over 100000 elements, the deflection value varies by only 0.05% over a difference of 618377 elements, and the bending stress by 0.02%, this suggests that the original simulation is mesh independent.

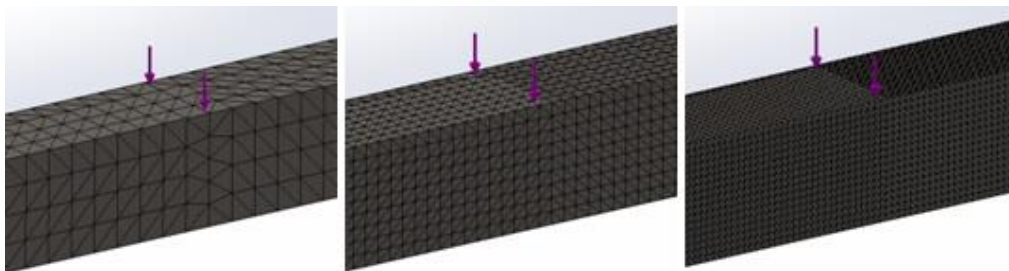
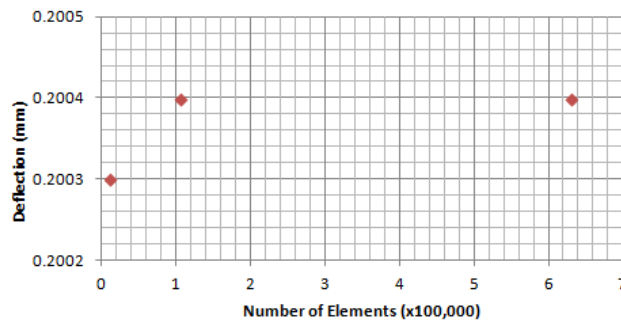


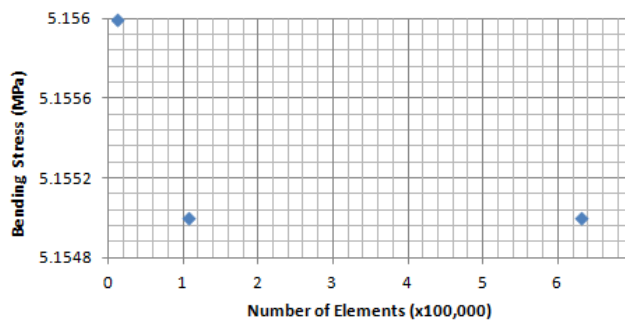
Figure 6: Global mesh refinement 20, 10 and 5mm elements respectively

Grid Dependency - Deflection



Graph 1: Graph of deflection against mesh elements showing mesh dependency.

Grid Dependency - Bending Stress



Graph 2: Graph of stress against mesh elements showing mesh dependency.

Validation Results

Values of shear stress and twist were compared against hand calculations to assess the accuracy and reliability of the models (Appendix 1).

The hand calculations and simulation results are in close agreement, with bending typically within 2% (Table 4) and torsion cases 5% (Table 5). However, the open section cases were closer to 10% out. This is partly due to the extent of deformation affecting measurements, and the calculated values are only accurate to 5% (Nisbett & Budynas, 2015). It is therefore considered that the simulations reflect reality within an acceptable margin of error.

Table 4: Bending Beam Results Comparison (2m beam under 1000N)

<i>Parameter</i>	<i>Source</i>	<i>Solid Section</i>	<i>Closed Section</i>	<i>Open Section C</i>	<i>Open Section U</i>	<i>Unit</i>
Bending Stress	Calculated	5.19	30.14	32.43	38.36	MPa
	FEA	5.155	28.8	28.59	36.62	
Deflection	Calculated	0.20	1.23	1.32	2.15	mm
	FEA	0.20	1.27	4.51	2.13	

Table 5: Beam Twist Results Comparison (2m beam)

<i>Parameter</i>	<i>Source</i>	<i>Solid Section</i>	<i>Closed Section</i>	<i>Open Section C</i>	<i>Open Section U</i>	<i>Unit</i>
Load	-	2000	2000	1	1	Nm
Shear Stress	Calculated	17.32	77.23	3.14	2.89	MPa
	FEA	18.80	85.00	3.00	2.89	
Angle of Twist	Calculated	0.44	2.75	2.23	2.02	mm
	FEA	0.45	2.88	2.03	1.92	

The Vitesses' main rails are constructed from two rolled steel 'C' sections nested and resistance spot welded (Fig.7). Short sections were modelled and it was found that incorporating weld nuggets slowed the solver and required more elements to effectively analyse. The FEA demonstrated less than 1% difference and so the joint is disregarded.

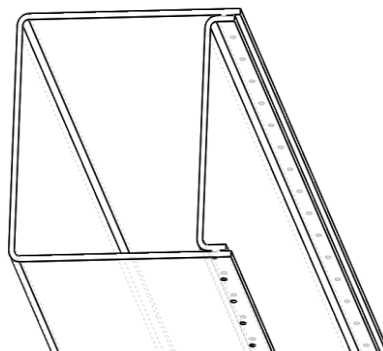


Figure 7: Chassis Main rail with spot welds

Chassis Structure

Model

The Spitfire chassis as tested by Pettifor (1991) was modelled first to get a valid baseline case. The chassis model was regularly tested (Fig. 8) against Pettifor's verified results, this both guided the model toward an accurate representation of the Spitfire chassis and showed which features had the greatest effect on chassis stiffness; this process is documented in Appendix 5.

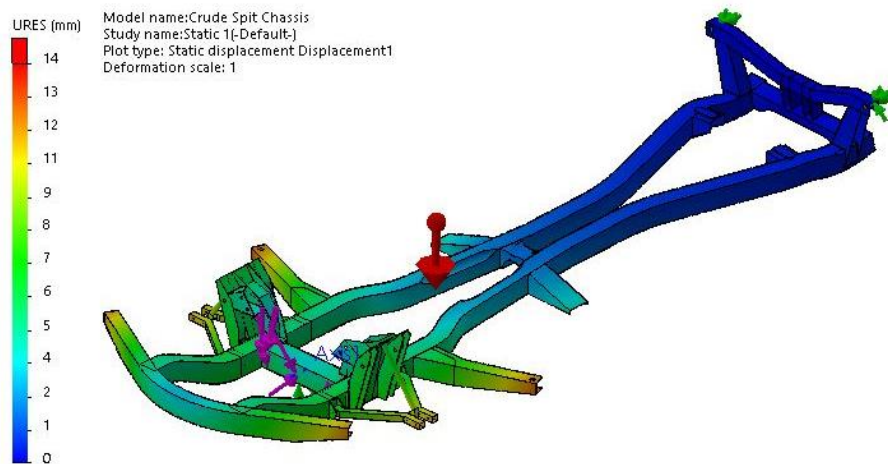


Figure 8: Spitfire chassis simulation, resultant displacement plot

The chassis model was created from dimensions and diagrams provided by Standard Triumph in their Service Training Notes (Standard Triumph, 1962). These diagrams were imported into Solidworks and scaled appropriately, features could then be added based directly off the factory drawings. Once the Spitfire chassis was modelled accurately and in reasonable agreement with Pettifor's results, the model was adapted to represent the Vitesse chassis (Fig. 9). This is documented at Appendix 6.

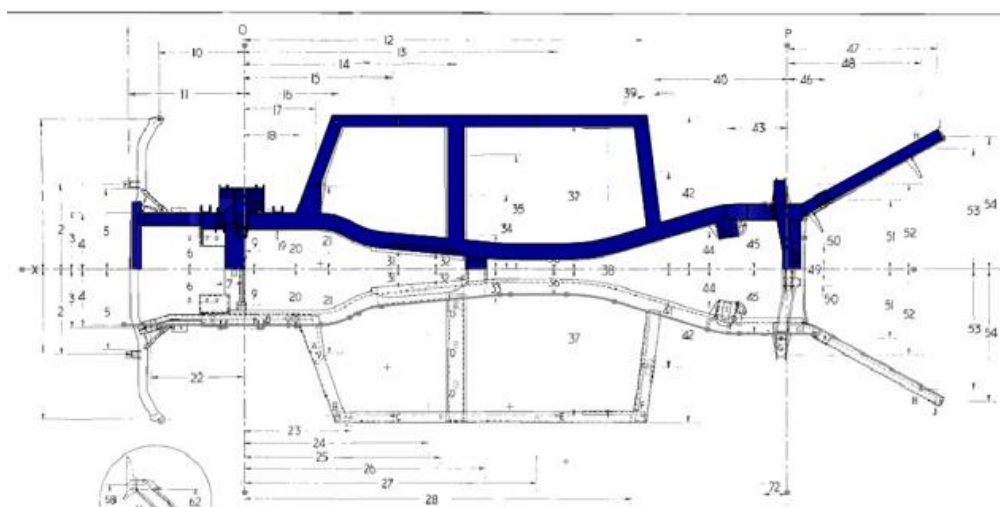


Figure 9: Vitesse chassis modelled on factory drawings

Fixtures

The chassis model was fixed at the rear damper mounts and movement was fixed in all axes but allowing rotation. The front was fixed at the front cross member using fixtures with 'reference geometry' as shown in Figure 10.

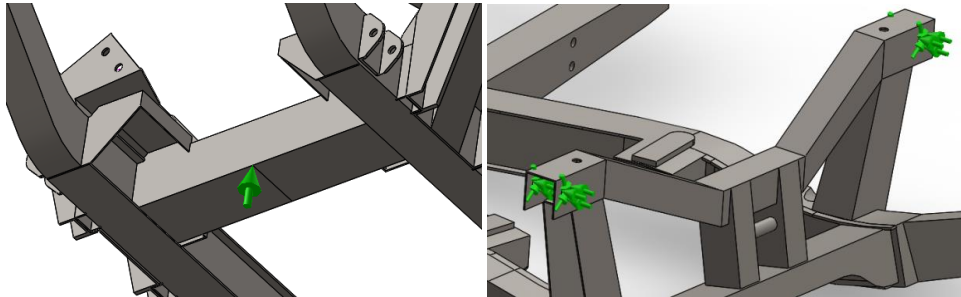


Figure 10: Vitesse chassis front and rear simulation fixtures

Loads

The load was initially applied as a torque of 1000Nm applied to the front face of the cross member and about an axis through the centre of the cross member. This was later amended to better represent the loads applied in testing and road use - forces of 1500N applied directly to the turret faces that react the front damper loads - equivalent to 1000Nm about the front cross-member (Fig. 11).

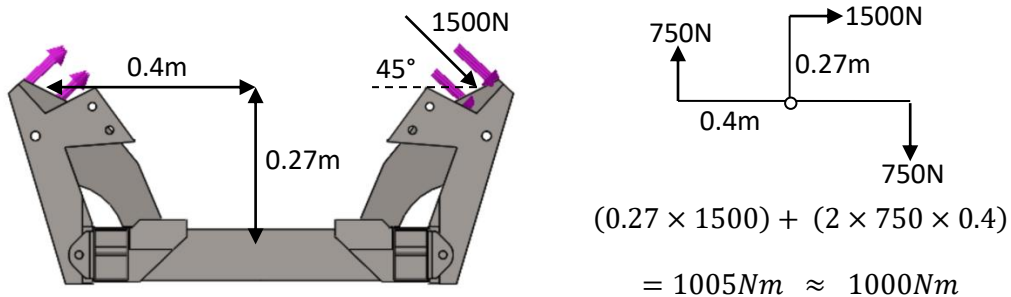


Figure 11: Vitesse chassis: load applied to front suspension turrets FBD

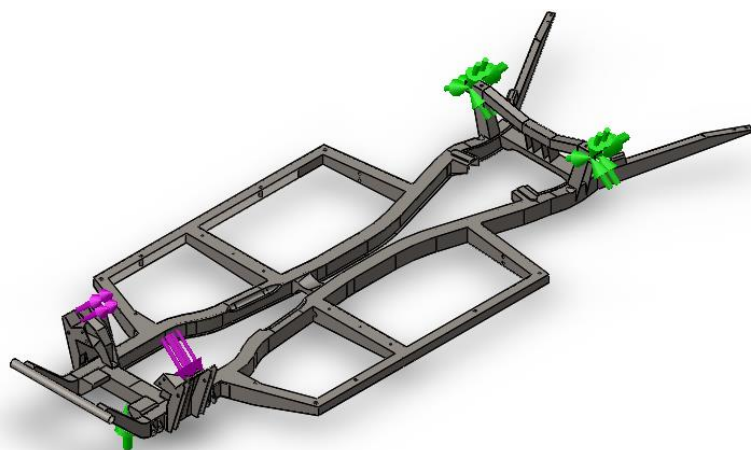


Figure 12: Chassis simulation layout as applied to all later vehicle structure simulations

Mesh

The curvature based mesh method was applied to the model. Here, the user may specify the maximum and minimum element size and the number of elements in a circle as well as the growth ratio. This allows the mesh to adapt to the structure being meshed, as in Figure 13; this is a more robust method and requires fewer mesh controls (Solidworks, 2013). Mesh independence was confirmed as described above, and the final mesh settings may be seen in Table 6.

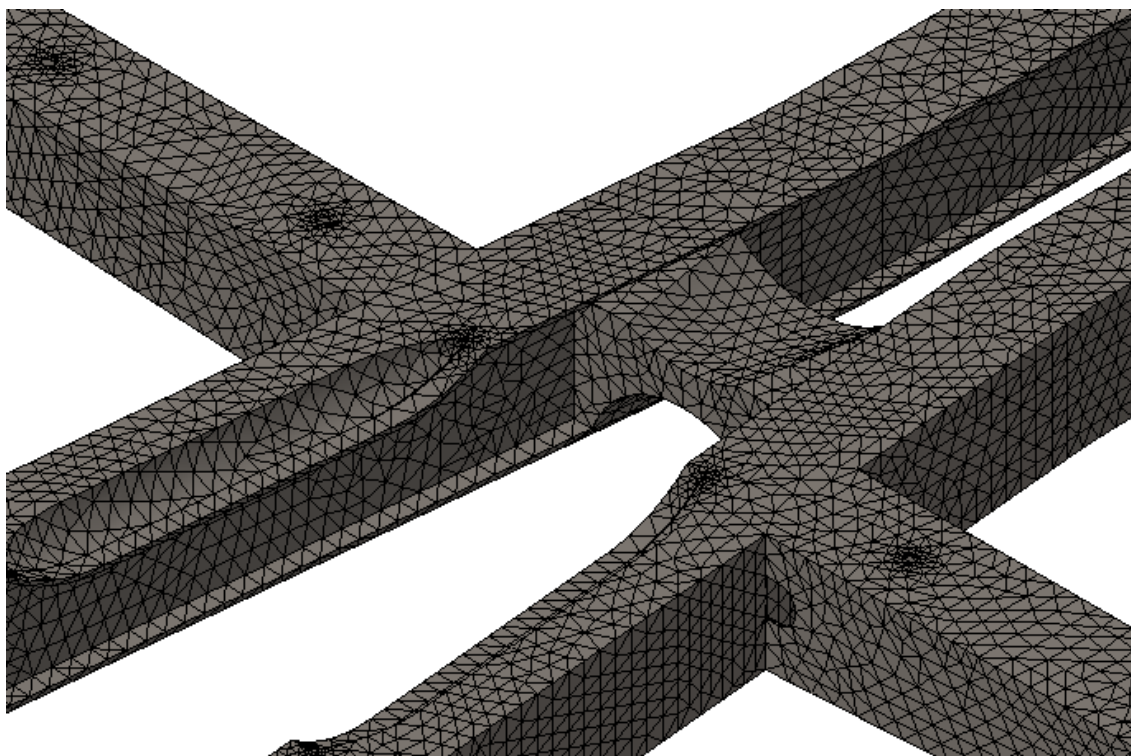


Figure 13: Curvature based mesh, showing variation in mesh density

Table 6: Final mesh settings applied to all simulations

Maximum Element Size:	12mm
Minimum Element Size:	2.4mm
Min No. of Elements in a Circle:	36
Element Growth ratio:	1.6

Solver

The simulation was solved using the iterative solver FFE Plus. This method assumes a solution and calculates associated errors. The solver continues to iterate and converges on a solution of acceptable accuracy as specified by the residual error stopping threshold.

It can be seen in Table 7 that the target stopping threshold was reached in 727 iterations, this can also be seen in Figure 14.

Table 7: Table of chassis simulation properties

Degrees of Freedom:	1541307
Number of Nodes:	513770
Number of Elements:	259530
Achieved Stopping Threshold:	9.92E-05
Target Threshold:	0.0001
Performed iterations:	727

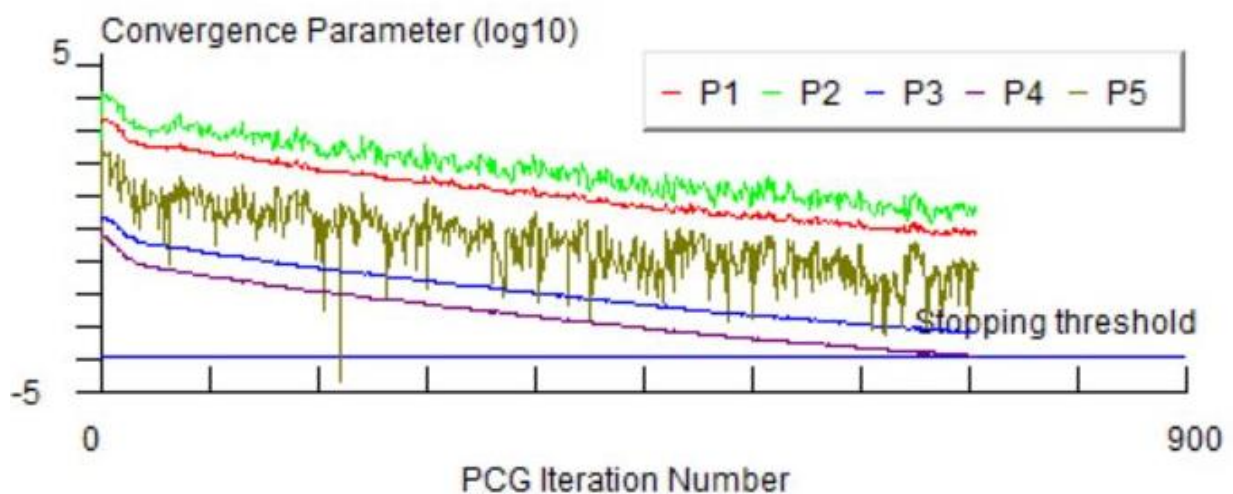


Figure 7.14: Chassis simulation convergence graph

- P1 – Reduction in 2-norm residual
- P2 – Reduction in infinity norm of residual
- P3 – Preconditioned norm of residual
- P4 - Normalized energy norm of error
- P5 – Difference in 2-norm residual

Post Processing

Vertical displacement was measured using Solidworks sensors (Fig. 15); this data was then used to calculate twist angle and stiffness, as shown later. Stress was also monitored to ensure the model behaved as expected (Fig. 16).

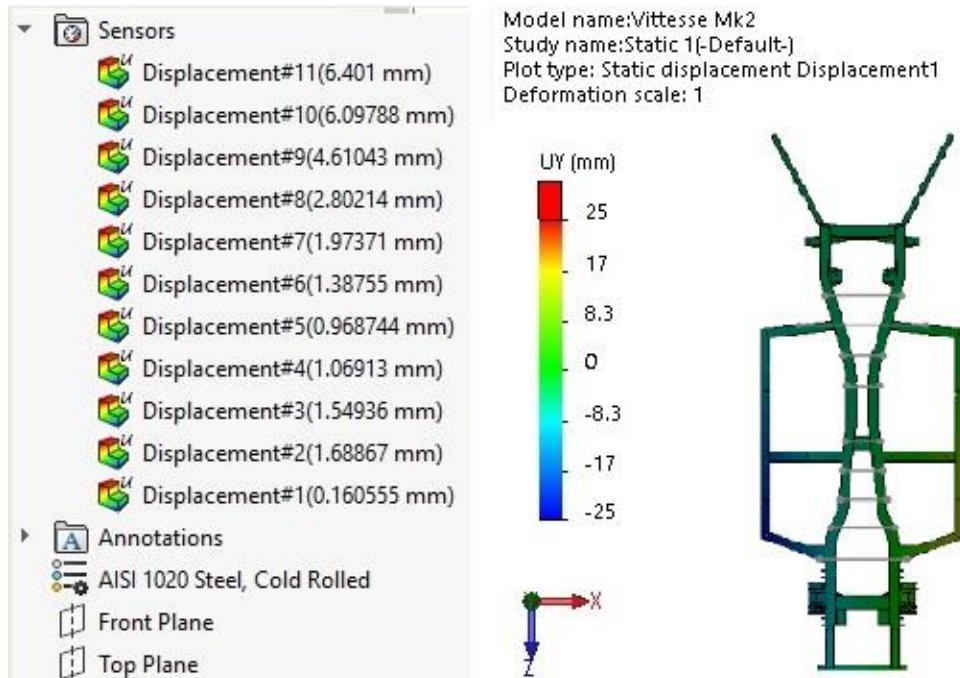


Figure 15: Chassis FEA sensor positions

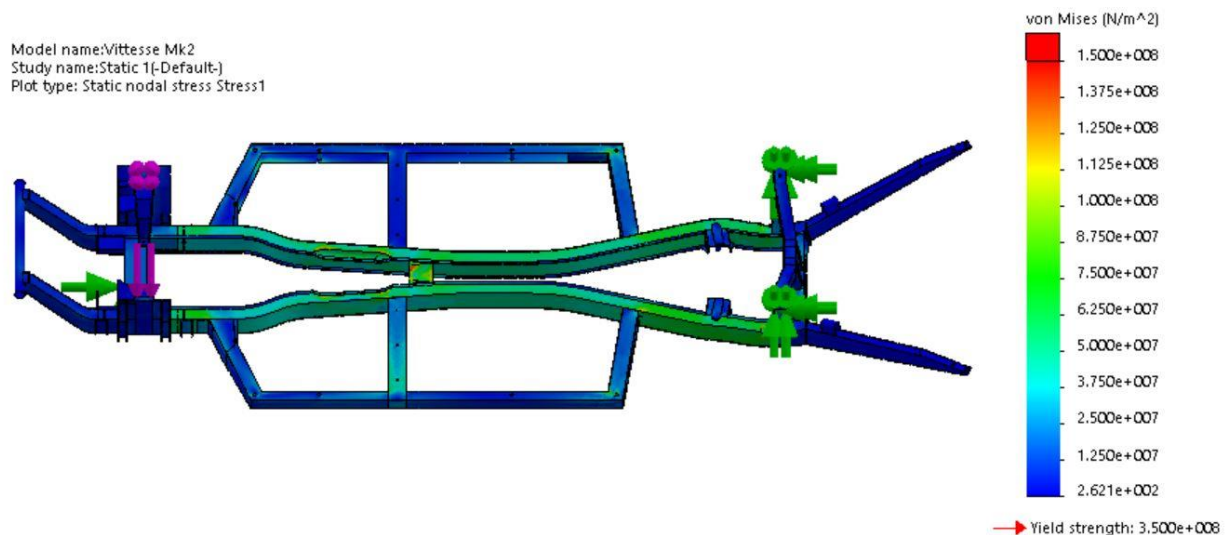


Figure 16: Chassis FEA Von Mises stress plot

Body Structure

The body structure was modelled from direct inspection and measurement of the test vehicle. The effects of the windscreen have been ignored since the screen is not bonded in place and is effectively rubber mounted.

The assembly model was setup as above, and bolted joints simulated using the Solidworks 'bolt' connection feature and 'no penetration contact'. Both FFE and large problem 'direct sparse' solvers were used, however both were aborted after 10 hours.

The assembly model was then combined into a part model and the chassis to body interface represented with extruded 'bolts' of 10mm diameter. This simplified the simulation, allowing it to be solved in less than one hour (Table 8), thus allowing rapid iterative changes and improvement in model accuracy, as well as later trial of multiple modifications within the project timescale.

Table 8: Table of vehicle body simulation properties

Degrees of Freedom:	7872834
Number of Nodes:	2624278
Number of Elements:	1336921
Achieved Stopping Threshold:	0.000106
Target Threshold:	0.0001
Performed iterations:	1443

A second simulation included doors, represented by solid bars linking the A and B pillars at the hinge and catch positions. Each run was logged at Appendix 7.

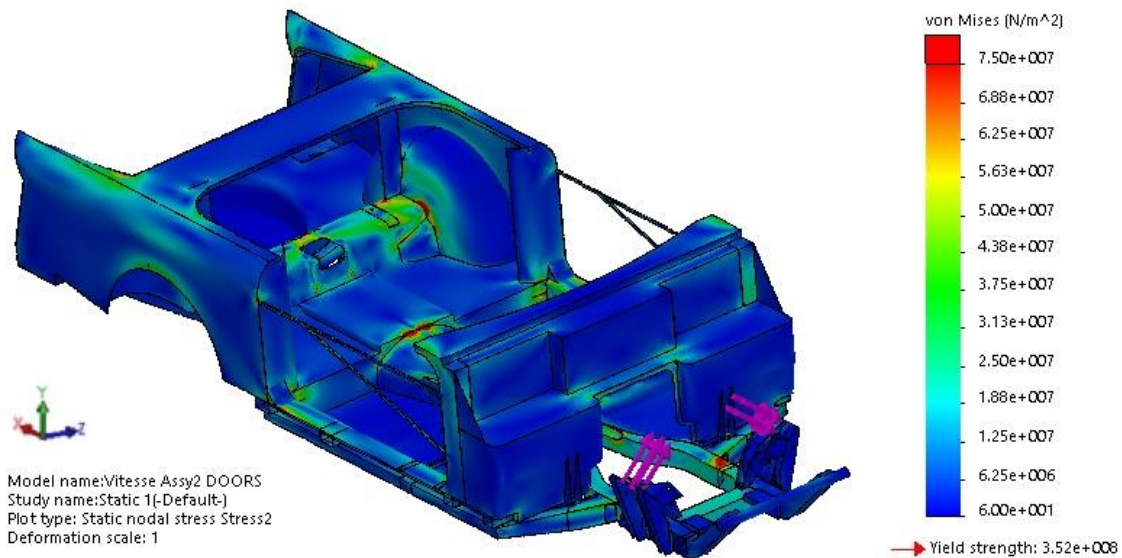


Figure 17: Vehicle body FEA Von Mises stress plot

Experimental Analysis

To verify the FEA, full scale physical testing was performed. This was carried out on a Triumph Vitesse Mk2 convertible in good structural condition. The structural configuration was standard; however the gearbox mount does not use the standard bolt in cradle. For a detailed account of the test method, layout and risk management see Appendices 8 - 11.

Test layout

The test vehicle was setup as in Figure 18. The vehicle was bolted to the floor using steel fixtures. The rear was fixed in all axes but allowed to twist about the fixture bolts (Fig.19), the front was supported vertically on a ball bearing and allowed to pivot (Fig. 20). Load was applied directly to the wishbone on one side and via a pulley on the other inducing a torque (Fig. 21).

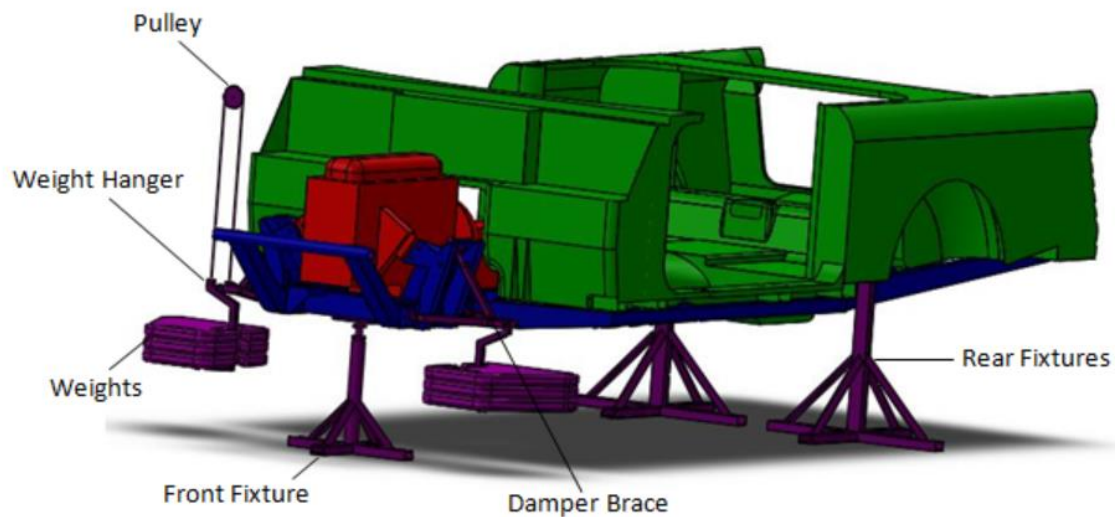


Figure 18: Experiment layout and test fixtures



Figure 19: LH rear fixture bolted to the floor and chassis damper mount



Figure 20: Front fixture detail

The front damper assembly was replaced with a rigid brace, and the rubber wishbone mounts were replaced with solid aluminium bushes (Fig.21).



Figure 21: Left and right front corners respectively, in test configuration

Chassis only tests were performed with the body in position but lifted clear on four scissor jacks. For the full structure tests, the body was mounted using metal spacers rather than the factory canvas and rubber pads, this may increase stiffness slightly but should simplify later analysis since linear behaviour is maintained. See Appendices 10 and 11 for details of fixtures and test photographs.

Measurement

Structural twist across the car was measured at 11 positions as in Figure 22. These positions were chosen to coincide with chassis features such as outriggers and sub-frame mounts to measure their effect. Distance between positions was measured using a tape measure and recorded.

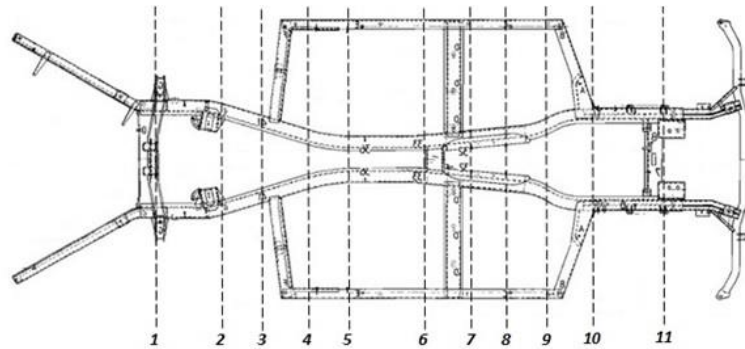


Figure 22: Experiment twist measurement positions

The twist angle was measured using the DC134 “Digital Level” manufactured by Fuzhou Yuxin Electronic Co Ltd, with a display resolution on $\pm 0.01^\circ$. Sections of 15mm copper pipe were glued to the bottom of the chassis to provide reliable datum points, and the angle measurements taken from a straight edge braced between them as in Figure 23.



Figure 23: Measurement method showing parallel bar and datum standoffs

All positions were measured in this way except position 11. In this case, the inclinometer was fixed directly to the front fixture plate as in Figure 24.



Figure 24: Position 11 twist measured directly off fixture plate

Test Method

Before each test, the structure was measured at every position with no load applied. The structure was then loaded incrementally up to the maximum test load and the unloaded in the same increments. At each increment measurements were taken twice to ensure consistency and generate an average. The tested vehicle was then reconfigured and tested again. See Appendix 8 for the full test setup and procedure.

Test Fixture Analysis

The rear fixtures were considered most susceptible to flexing due to their greater unsupported length. This was tested by mounting a laser level to the top of the fixture and projecting the line onto the workshop wall, the line was then marked and the vehicle structure loaded to its maximum test load of 1700Nm. No deflection was observed compared to the marked un-laden position.

The resolution of this method was calculated as in Figure 25. It can be seen that 1° of flex at the fixture manifests as 21.8mm measured displacement across the width of the car (twist), and 3.8mm measured displacement down the car (bending). The front fixture was considered not to flex since its size and geometry makes it inherently stronger than the proven rear fixtures.

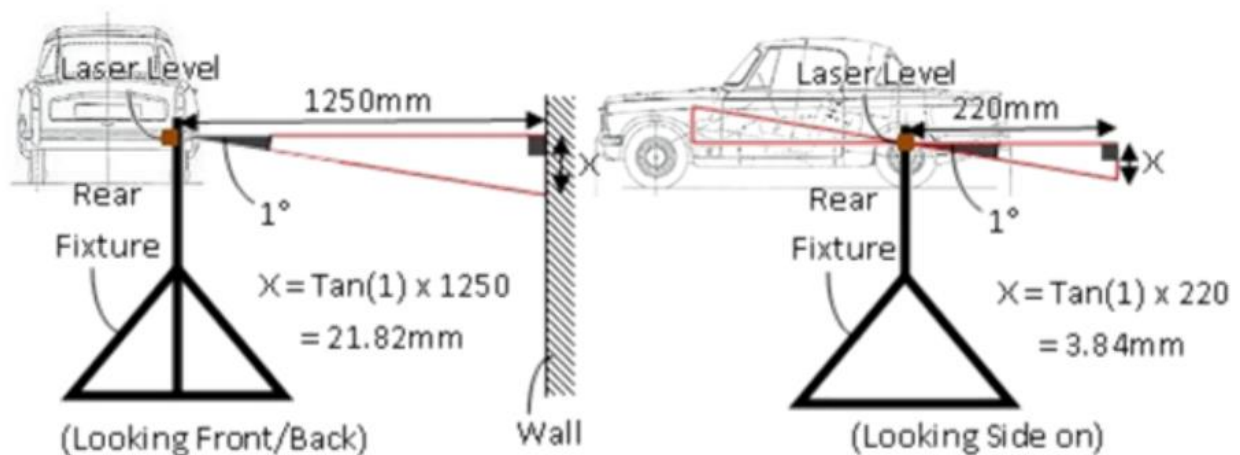


Figure 25: Rear fixtures laser level deflection resolution calculations

Modifications

The modifications considered are for a road vehicle, so must have minimal effect on the practical use of the vehicle; in passenger access, ground clearance and maintenance. See Appendix 14 for a full specification.

As discussed above, for the greatest effect any additional structures should increase the I_z and be situated as far from the vehicles neutral axis as is possible, since I_z is dependent on the square of this distance. Therefore the most effective additions would be a roof and or a full roll cage, however these are ruled out in the specification.

Various modifications to chassis and body were tested; these may be seen in Appendix 20 and in the FEA logs in Appendices 18 & 19. In order to ensure the model responded to modification as the real structure would, two modifications were made and tested on the bare chassis as above.

First, the original side-rails were replaced with 50x50x2mm steel box section and the front outriggers closed with 1.2mm steel plate. The new side-rails were reinforced, as shown in figure 26, since the originals had cracked around the body mounts. Since this is now a closed section, drain holes were added to reduce the speed of corrosion.

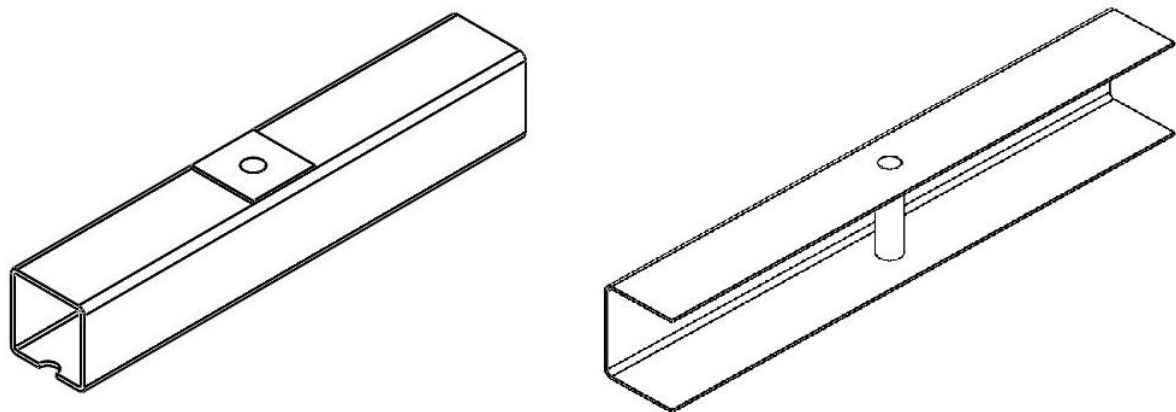


Figure 26: New side-rail (Left) compared to old (Right)

Second, a bolt-in cross-member was fabricated from 50x30x3mm box and 6mm plate, and mounted 340mm back from the middle cross-member, as in figure 27. It was necessary for this to be a bolt-in feature in order to keep access to the prop-shaft.

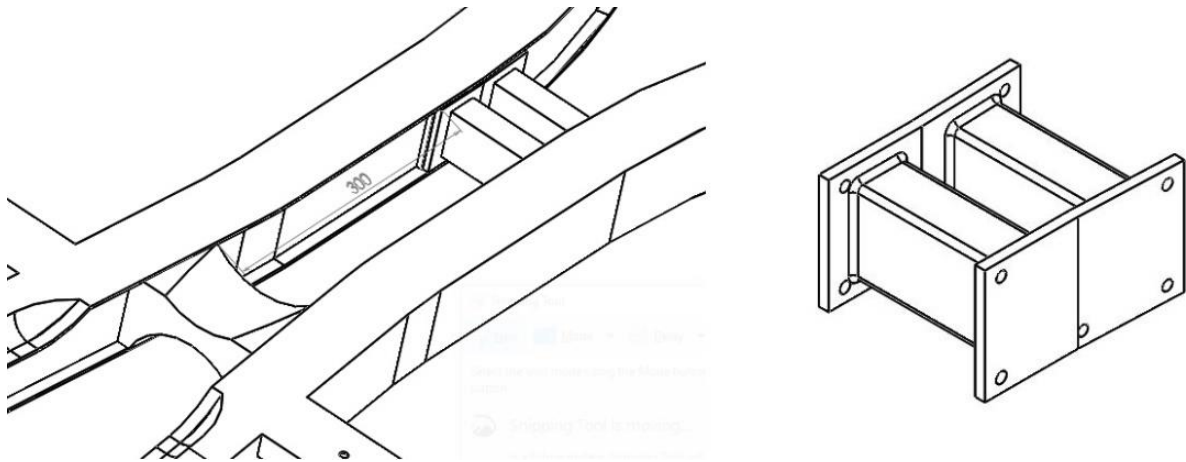


Figure 27: Second cross member fitted 340mm back from middle cross member.

These modifications were replicated as closely as possible in Solidworks and subjected to FEA as before – see figure 28 and Appendix 18 for details.

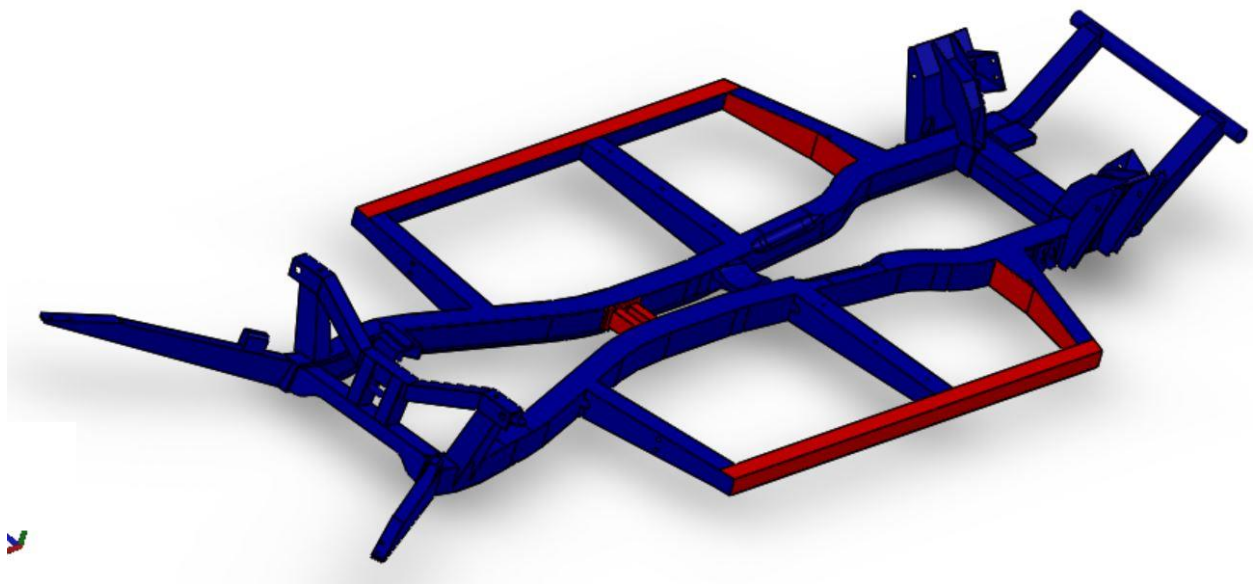


Figure 28: Tested modification configuration (red)

Results

Solidworks FEA Results

Solidworks sensors were used to measure the Y displacement (x) at each station. The distance from the 'neutral axis' to the measured point (d) was used to calculate the angle of twist:

$$\theta = \text{Sin}^{-1}(x/d) = \text{Sin}^{-1}(6.5/336) = 2.22^\circ \quad [10.1]$$

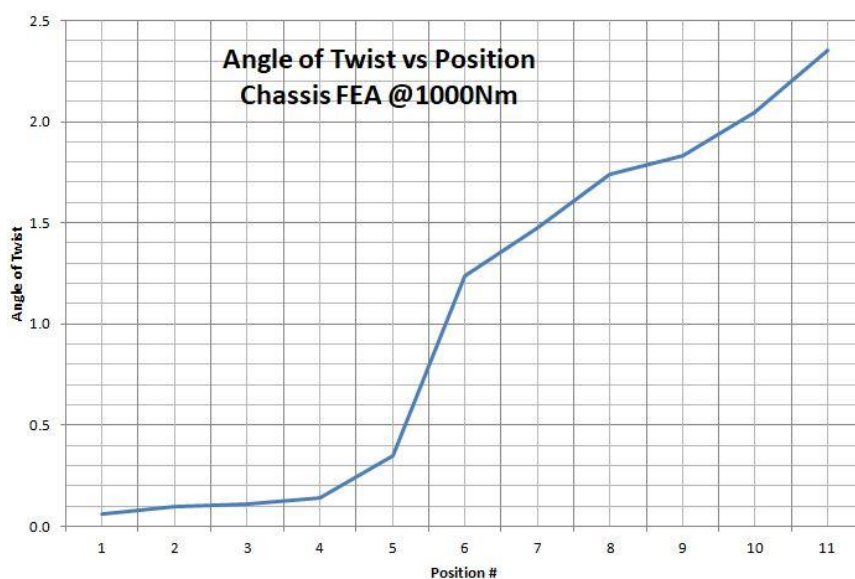
Table 9: Chassis FEA calculated twist angles at 1000Nm applied load

Chassis FEA Position #	Distance d mm	Disp. x mm	Twist θ °
1	446.4	0.23	0.06
2	380.6	0.33	0.10
3	257.8	0.25	0.11
4	136.0	0.17	0.14
5	92.0	0.28	0.35
6	113.4	1.22	1.23
7	152.0	1.96	1.48
8	188.3	2.86	1.74
9	291.4	4.65	1.83
10	336.0	6.00	2.05
11	336.0	6.90	2.35

*At 1000Nm

The calculated angle of twist was then used to calculate torsional stiffness as in equation 3:

$$k_\theta = \frac{T \times l}{\theta} \quad e.g. \frac{1000Nm \times 2.5m}{2.22^\circ} = 1116 (Nm/^\circ)/m \quad [10.2]$$



Graph 3: Chassis FEA: sensor position against twist angle

Experimental results

The experimental data (Appendix 12) was processed in Microsoft Excel (2007). The measured twist was averaged and corrected against zero load measurements.

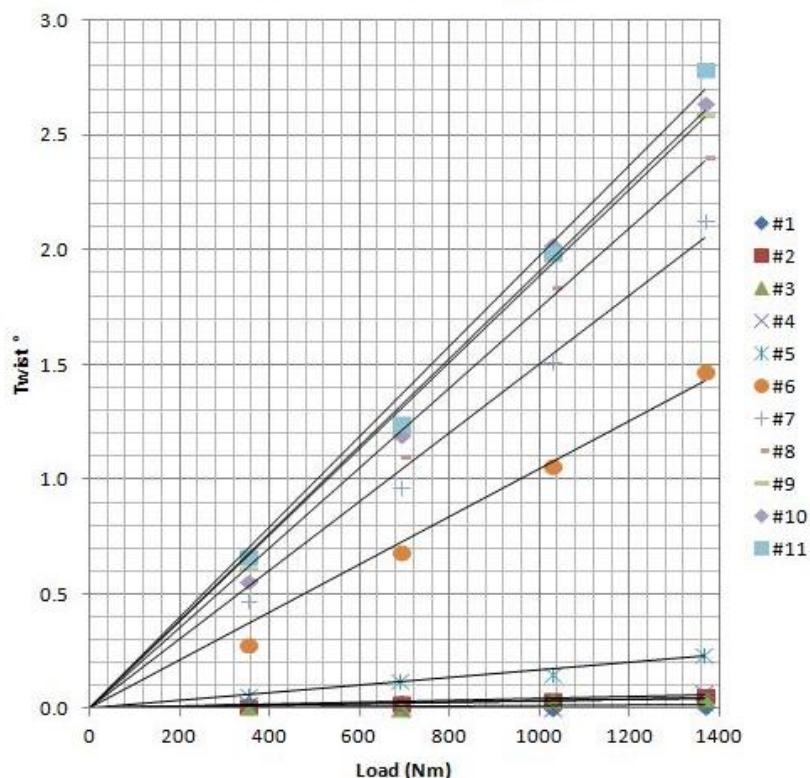
Table 10: Chassis experiment: averaged angle of twist

Posn #	Twist Angle ($\pm 0.1^\circ$) at Load (Nm)			
	352.85	691.35	1028.44	1367.15
1	0.03	0.03	0.00	0.01
2	0.02	0.03	0.05	0.06
3	0.01	0.01	0.04	0.05
4	0.03	0.01	0.01	0.08
5	0.06	0.13	0.16	0.24
6	0.29	0.69	1.07	1.47
7	0.47	0.97	1.51	2.13
8	0.57	1.11	1.84	2.41
9	0.62	1.21	2.00	2.60
10	0.56	1.20	2.03	2.64
11	0.67	1.25	1.99	2.79

*Data collated from experimental loading data.
Used to plot graph of Twist vs Load

Corrected twist values were plotted for each measured station against the torque load applied. This showed the behaviour to be linear, as expected. A linear trend-line was added for each series and forced through zero as it was assumed the response remains linear to zero.

Load vs Twist Angle



Graph 4: Chassis test load against angle of twist at each position

The gradient of the trend-line was then used as a coefficient to calculate 'accurate' twist values for regular applied loads and these values used to calculate torsional stiffness per section as well as overall stiffness:

$$\theta = Xcoefficient \times T \quad e.g. \quad 0.001972 \times 1000Nm = 1.972^\circ \quad [10.3]$$

$$k_\theta = \frac{T \times l}{\theta} \quad e.g. \quad \frac{1000Nm \times 2.46m}{1.972^\circ} = 1247.45 (Nm/^\circ)/m \quad [10.4]$$

Table 11: Chassis experiment: corrected angle of twist

xcoefficient	Twist Angle (°) ±4.5% at Load (Nm)						
	400	600	800	1000	1200	1400	1600
-							
0.000013707	0.005	0.008	0.011	0.014	0.016	0.019	0.022
3.10674E-05	0.012	0.019	0.025	0.031	0.037	0.043	0.050
3.44891E-05	0.014	0.021	0.028	0.034	0.041	0.048	0.055
4.37322E-05	0.017	0.026	0.035	0.044	0.052	0.061	0.070
0.000170103	0.068	0.102	0.136	0.170	0.204	0.238	0.272
0.001043448	0.417	0.626	0.835	1.043	1.252	1.461	1.670
0.001502137	0.601	0.901	1.202	1.502	1.803	2.103	2.403
0.001742709	0.697	1.046	1.394	1.743	2.091	2.440	2.788
0.001884629	0.754	1.131	1.508	1.885	2.262	2.638	3.015
0.001902846	0.761	1.142	1.522	1.903	2.283	2.664	3.045
0.001972025	0.789	1.183	1.578	1.972	2.366	2.761	3.155

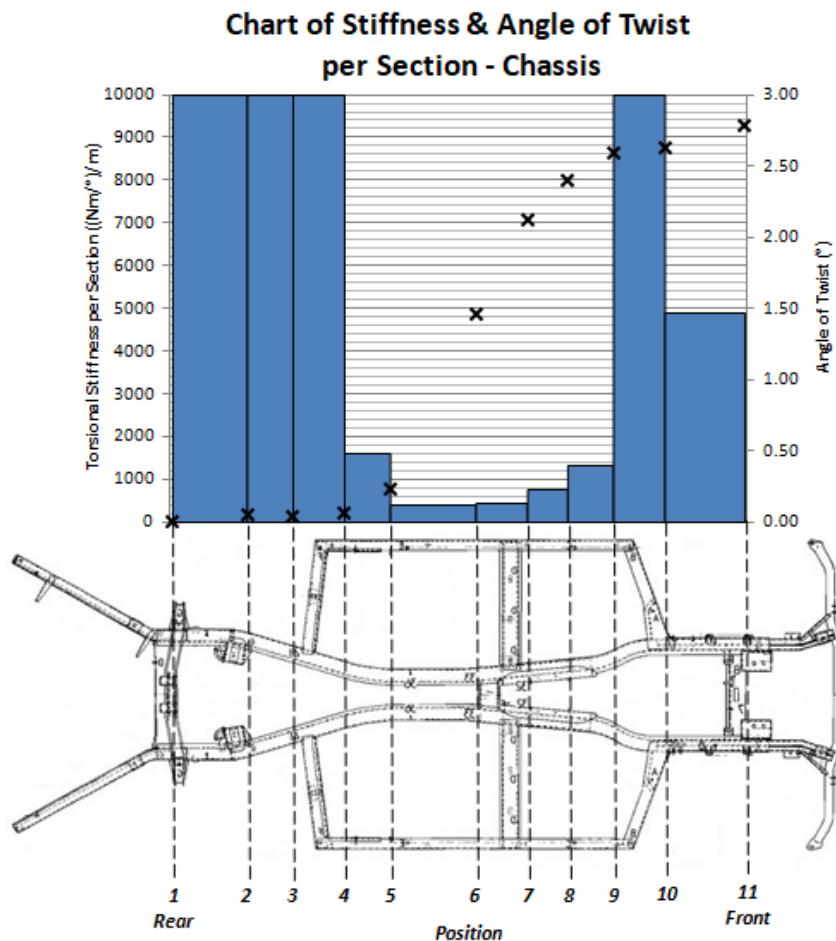
*Values calculated from trendline coefficients to find 'accurate' twist angles

Table 12: Chassis experiment: calculated torsional stiffness per chassis section

Posn #	Section Length(mm)	Torsional Stiffness ((Nm/°)/m) at Load (Nm)							Average
		400	600	800	1000	1200	1400	1600	
1	N/A	N/A	N/A	N/A	N/A	N/A	N/A	N/A	N/A
2	336	19354.39	19354.39	19354.39	19354.39	19354.39	19354.39	19354.39	10000.00
3	204	59619.49	59619.49	59619.49	59619.49	59619.49	59619.49	59619.49	10000.00
4	207	22395.08	22395.08	22395.08	22395.08	22395.08	22395.08	22395.08	10000.00
5	207	1638.04	1638.04	1638.04	1638.04	1638.04	1638.04	1638.04	1638.04
6	372	425.95	425.95	425.95	425.95	425.95	425.95	425.95	425.95
7	202	440.39	440.39	440.39	440.39	440.39	440.39	440.39	440.39
8	190	789.78	789.78	789.78	789.78	789.78	789.78	789.78	789.78
9	192	1352.87	1352.87	1352.87	1352.87	1352.87	1352.87	1352.87	1352.87
10	210	11528.01	11528.01	11528.01	11528.01	11528.01	11528.01	11528.01	10000.00
11	340	4914.79	4914.79	4914.79	4914.79	4914.79	4914.79	4914.79	4914.79
Overall	2460	1247.45	1247.45	1247.45	1247.45	1247.45	1247.45	1247.45	1247.45

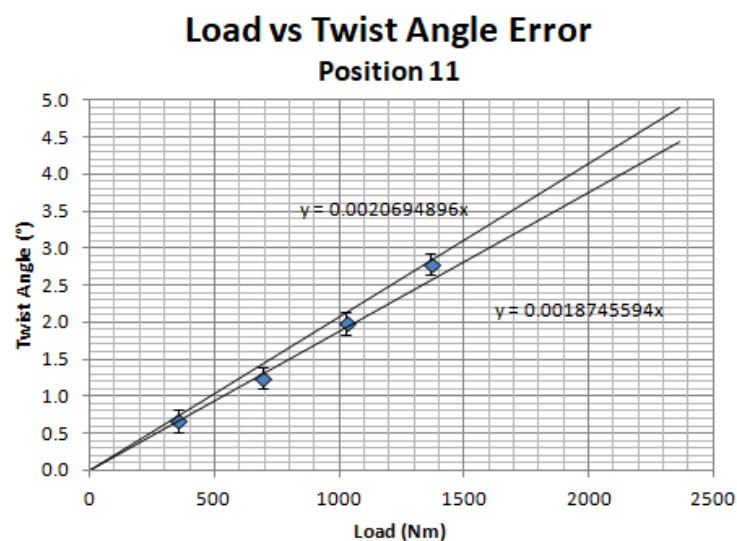
*Values calculated from cacluated twist to generate accurate stiffness values

Averaged stiffness capped at 10000 (Nm/°)/m to improve chart resolution



Graph 5: Chassis experiment: torsional stiffness per section

Error was calculated by plotting a linear trend-line through the extremes of the ± 0.1 error bars and using the coefficient to calculate twist, thus torsional stiffness at each extreme as detailed above. This produced an upper and lower magnitude of stiffness from which percentage error was calculated.



Graph 6: Chassis experiment: applied load against maximum and minimum twist uncertainty

Further calculations and processed results may be seen at Appendix 13.

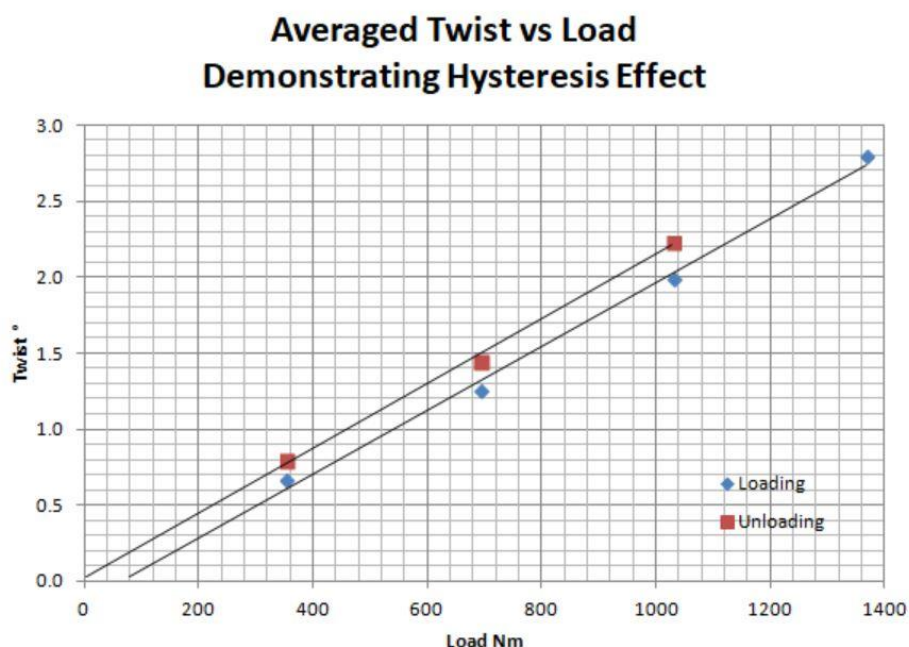
Modification Results

The same method was applied to modification data at Appendix 16 and 17.

Discussion

Each data set took one hour to collect under the vehicle hence human error is likely a large factor. In addition, the inclinometer used in testing specifies a repeatability of only $\pm 0.1^\circ$. Despite this, the standard deviation of the raw data collected is typically under 0.05° . To account for this and error in distance measurements, an uncertainty of $\pm 0.1^\circ$ was used to calculate uncertainty.

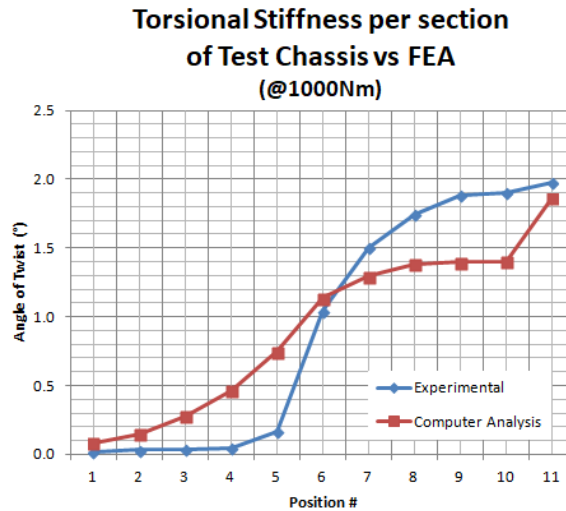
Zero readings were taken before and after loading, these readings can be seen to return to the same point within the measurement error of $\pm 0.1^\circ$, so within the uncertainty of the experiment, the structure returned to zero. This hysteresis effect, seen in Graph 7, is present in all data sets. This could be due to slack in the experiment setup since 80N of preload is required before any twist is measured, or hysteresis in the joints of this complex structure.



Graph 7: Chassis loading and unloading data showing hysteresis

The angle of twist was calculated by averaging the twist readings and subtracting the averaged zero reading; this yielded twist angles between 0° and 3° . Therefore a repeatability of 0.1° is a significant percentage error; particularly as both the zero and twist measurements have this attached uncertainty. This could have been reduced by increasing applied load during testing to induce a greater twist, and reduce the percentage error, though at the risk of permanent structural deformation. Where the displacement was smaller than the resolution of the inclinometer used, the difference in twist between stations was sometimes very small or negative. This is likely erroneous, since calculated stiffness then trends toward infinity. Since this study is primarily interested in weak areas of the structure, averaged stiffness values were capped at $10,000\text{Nm/deg}$.

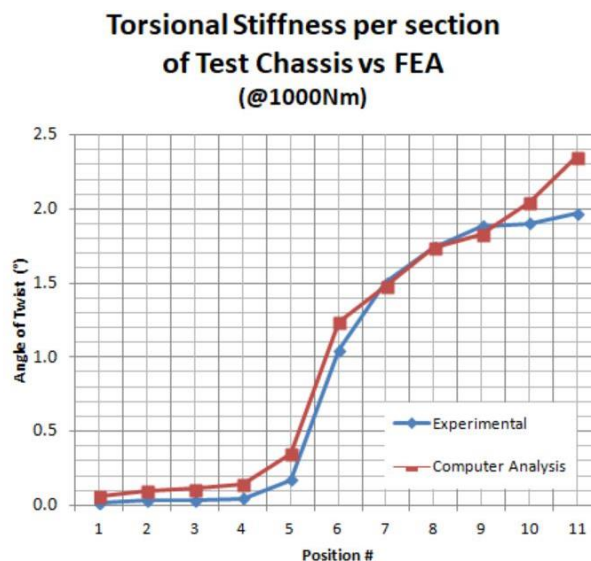
A feature that appears in some of the data sets is an apparent reduction in stiffness at the front of the vehicle between stations 10 and 11. This may be due to measurement error as explained above, particularly since station 11 was measured differently. Though this feature was considered erroneous, the FEA analysis demonstrates the same change in stiffness, as can be seen in graph 8. This suggests the apparent reduction in stiffness is real, though likely not to the extent indicated.



Graph 8: Comparison of experimental and FEA derived twist

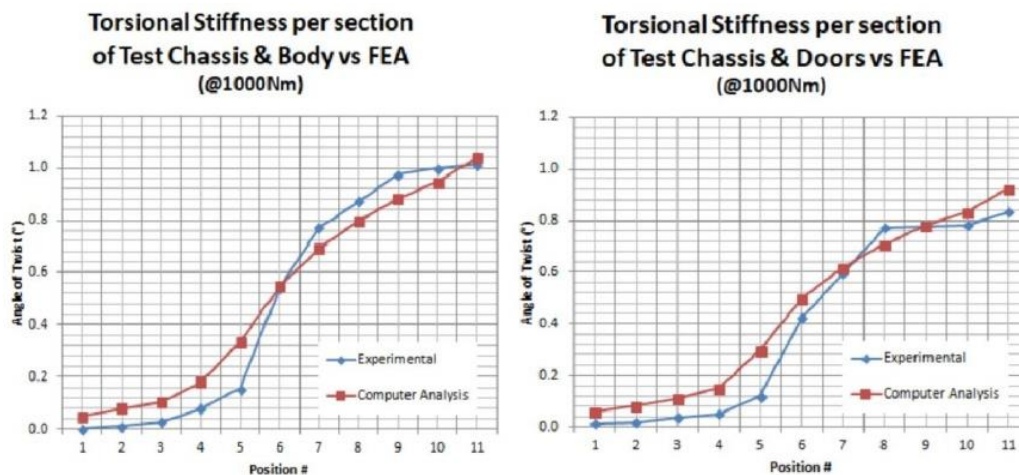
Graph 8 shows how the cumulative angle of twist along the chassis for both the experiment and the FEA model. The gradient indicates stiffness - a shallow gradient indicates smaller deflection for the specified load and hence a stiffer section. Though the FEA and experiment show similar overall stiffness the actual distribution of stiffness is not accurately represented. The experiment confirmed the structure responds linearly (Graph 7) and this was further confirmed in a non-linear FEA which yielded the same results as the linear-static study.

The simulated load was changed to more accurately reflect experimental loading conditions, as discussed above. Graph 9 shows the difference this loading case made; the fit is now much closer, particularly up to position 9.



Graph 9: Comparison of experimental and updated FEA derived twist

From 9-11 the structure appears less stiff than the test chassis, possibly due to extra structures in the chassis, such as the steering-rack and radiator (which were present though loosened), which are not accurately represented in the model. Graph 10 shows a similar effect on the assembly models, though the fit is acceptable.



Graph 10: Comparison of experimental and FEA derived body twist

The FEA twist measurements are calculated from vertical displacement, and the distance from the neutral axis. The neutral axis is assumed to be down the centre of the vehicle at the chassis top surface, however it is likely this axis angles up from the front pivot toward the rear fixtures. This would introduce an error into FEA twist, particularly in the body case.

Despite this, the FEA has an overall stiffness within 12% of the test chassis and is a close match in the areas targeted for modification, thus the model is considered valid. It should also be noted however that the gradient 6-7 is much shallower in the FEA, indicating it is stiffer in the model than real life. This is likely because the model does not accurately represent the joints in the real chassis, and may partially explain why the predicted performance of modifications was lower than that achieved.

Table 13: Overall torsional stiffness of vehicle structures

Test Configuration	Torsional Stiffness (Nm/°)/m	Increase in Stiffness %	Cumulative Improvement %
Chassis	1250 ±55 (5%)	-	-
+Engine	1280 ±60 (5%)	2%	2%
+Body	2450 ±180 (8%)	91%	96%
+Doors	2950 ±250 (9%)	20%	136%
+Roof	3550 ±450 (13%)	20%	184%
+Seatbelt Mounts	3420 ±350 (10%)	4%	174%

* +Component is cumulative e.g. +Body includes Chassis and Engine.

The experimental result of chassis stiffness is within the expected ballpark; 1250Nm/deg is close to that of the Spitfire chassis measured by Pettifor (1225Nm/°) (1991). This suggests that the main rails are doing most of the work and the side-rail structures have very little effect, despite being further from the neutral axis.

With the engine fitted, stiffness increased by approximately 30Nm/deg, however the uncertainty is $\pm 60\text{Nm}/^\circ$ on both the bare chassis and engine test and so this result is insignificant. FEA analysis of engine fitment suggests that the weight has minimal effect, probably because it is central. The engine and gearbox was also simulated as a series of rigid links and found to increase stiffness by 40%. The rigid links do not accurately represent the rubber mounted assembly, however it does suggest that a reinforced gearbox tunnel and turret braces could have a significant effect on stiffness.

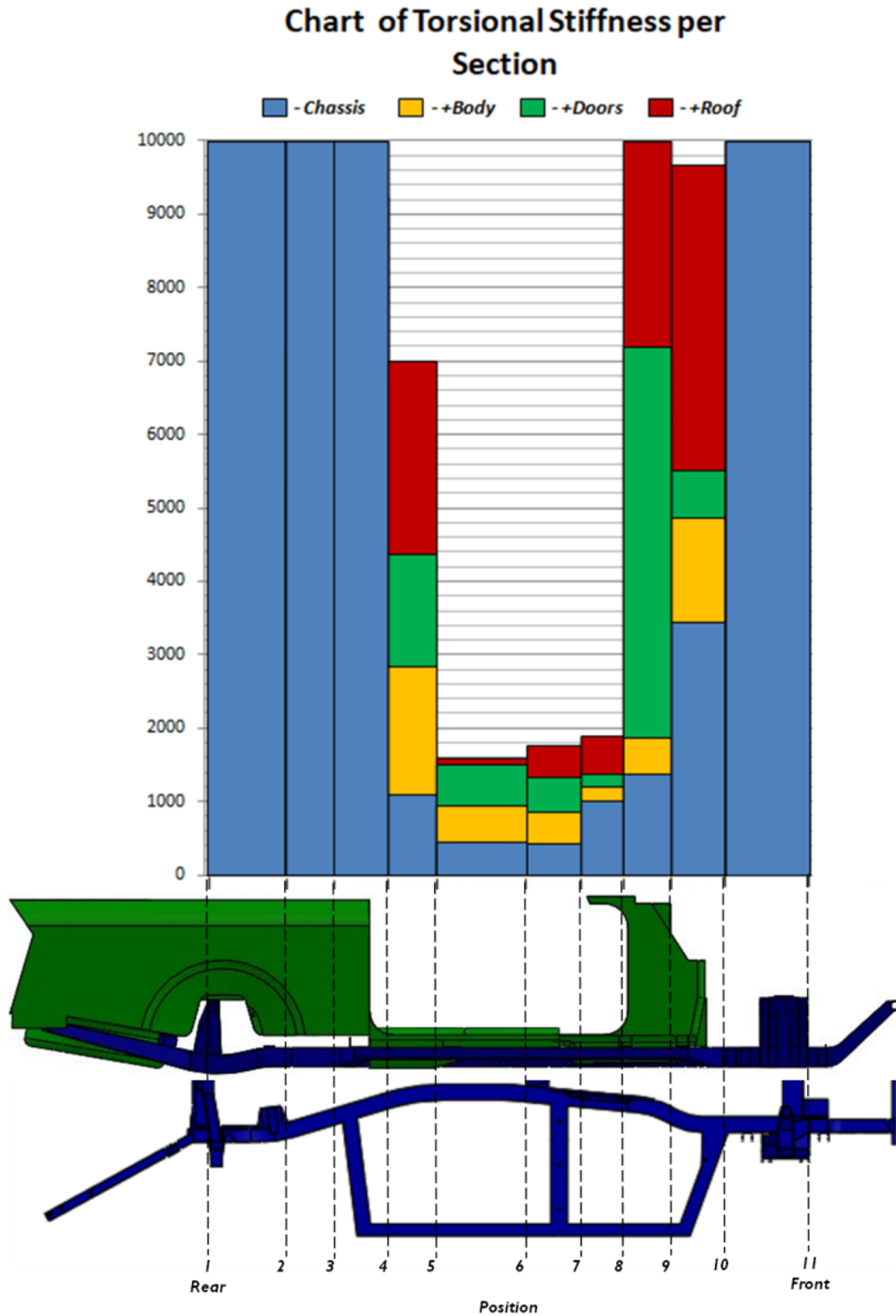
From the experiment, it can be seen that the body assemblies increase overall stiffness by 96%. This is expected, as the body links the corners of the side-rails across the car, reducing the degree of twist.

The FEA of the body structure and chassis agreed with the experiment within 5%. This is within experimental uncertainty and so can be considered a valid model. This may be a slightly artificial result since the body and chassis are simulated as a single part, rather than an assembly, with the interface represented by extruded 10mm 'bolts'. It was found that the stiffness of the model could be steered into the expected range by varying 'bolt' diameter. This shows the importance of the body/chassis interface. It would be more telling to validate the simulation of a body modification, to ensure the model reacts as expected.

The doors increase stiffness by 20%, and the roof by a further 20%. This is surprising since the roof is a folding structure covered by fabric, and bracing to the relatively weak windscreen pillars. However, the roof is tight, potentially preloading joints that would otherwise flex, and due to the distance from the neutral axis, I_z is increased significantly.

The seatbelt mounts tested are close to the neutral axis and so have minimal effect. The configuration is otherwise a repeat of the '+roof test' and the result falls within 4%, well within experimental uncertainty suggesting good repeatable data. Additionally, the seatbelt test was conducted with 5 weights and should be more accurate - increasing confidence that the 4 weight data is of comparable accuracy.

Graph 11.6 shows that the weakest area of the structure is at the door apertures and where the main rails are closest together; this is expected since I_z is at its lowest. Individual sectional stiffness charts may be found at Appendix 13.



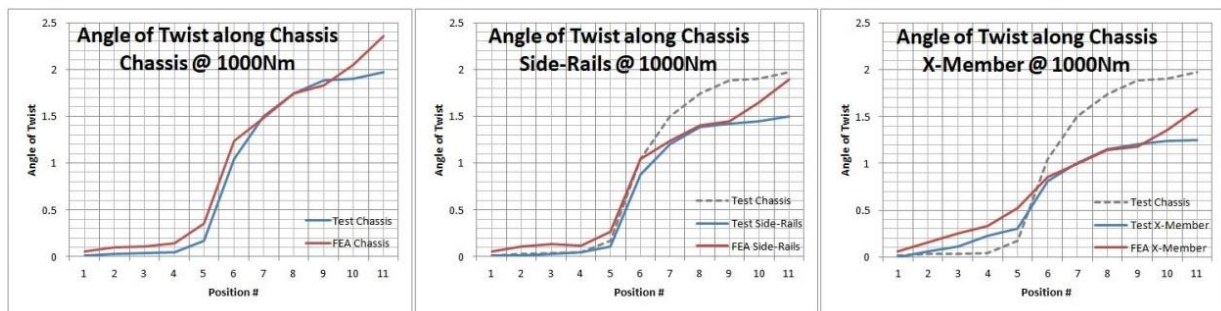
Graph 11: Comparison of sectional stiffness of structural elements

Table 14: Overall torsional stiffness of modified structures

Test Configuration	Torsional Stiffness (Nm/°)/m	Increase in Stiffness %	FEA Predicted Stiffness %
Chassis	1250 ±55 (5%)	-	-
+ Boxed SideRails	1640 ±90 (6%)	24%	19.3%
+2nd CrossMember	1950 ±140 (7.5%)	19%	30.8%
Complete Body	3550 ±450 (13%)	-	-
Body with Mods	4000 ±500 (14%)	13%	-

* +Component is cumulative e.g. +Body includes Chassis and Engine.

The modification experiments show the side-rails increased stiffness by 24%, and combined with the second cross-member an increase of 37% over the bare chassis, for an 8% (7kg) increase in weight. This improvement was measured as a 13% increase in stiffness on the assembled vehicle with the roof up. The uncertainty in this result overlaps with the 14% uncertainty of the comparative baseline result, and so it is marginal whether this is statistically significant. However, since the chassis tests proved a comparable magnitude stiffness gain, this can be considered reliable.



Graph 12: Validation of modification FEA results against experiment values

The FEA predictions of modification performance are close to the experimental findings, falling within the margin of experimental uncertainty. Graph 11.6 shows how closely the FEA predictions match the actual results obtained. This further validates the model and increases confidence in the predicted performance of other modifications simulated (See appendices 17 & 18).

The FEA results include stress distribution across the structure. This was used to track the migration of stress concentrations as modifications changed local stiffness. Care was taken to identify singularities – areas of infinitely high stress artificially induced by the resolution of the mesh. This can be checked by progressively refining the local mesh and observing if the stress plateaus or continues to increase. In Figure 29, stress concentrations appear where expected, though concentrations around fixtures are considered unreliable.

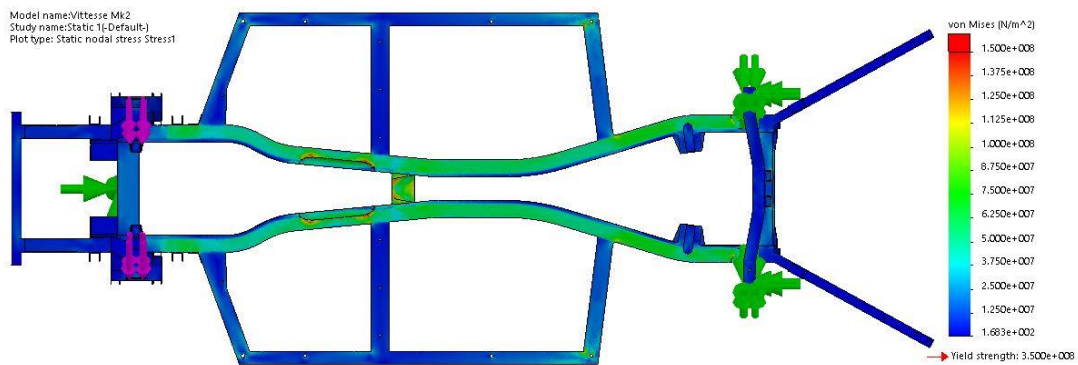


Figure 29: Von Mises Stress plot of the standard Vitesse chassis at 1000Nm

Figure 30 demonstrates how the modifications tested change the stress distribution in the chassis. It can be seen that the main rails are less stressed and the load is distributed more evenly through the outriggers and side-rails.

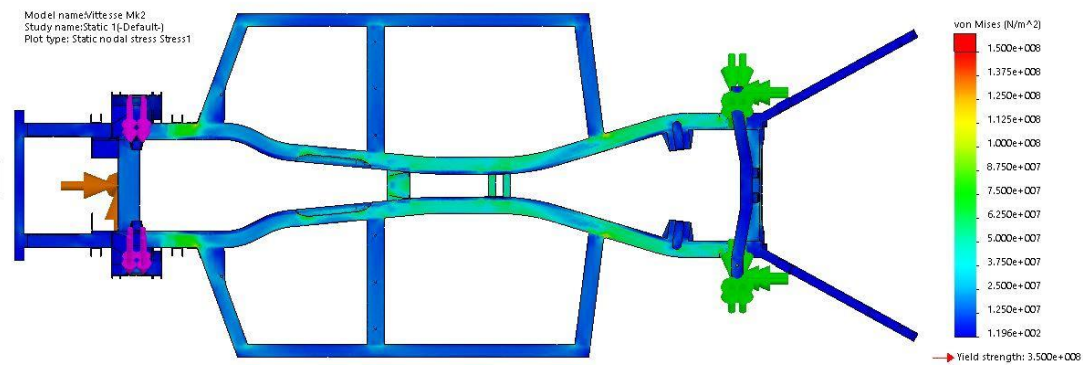


Figure 30: Von Mises Stress plot of the modified Vitesse chassis at 1000Nm

The main rail ahead of the front outrigger joint is of interest since, on the stiffer GT6 and vehicles with roll cages, these areas have been known to crack (Sideways, 2015). These fatigue cracks are caused by cyclic stresses above the endurance limit of the material.

The endurance limit of steel is $0.5 \times$ tensile strength ($< 1400\text{MPa}$) (ASM International, 2008), and the AISI 1020 steel simulated has a tensile strength of 420MPa , hence an endurance limit of 210MPa . Figure 32 shows the body simulated with pseudo roll cage, increasing stiffness to 6600Nm° . The FEA demonstrates the endurance limit of the material is not exceeded, therefore the modifications proposed should not reduce the structures fatigue life. Comparing Figures 31 and 32, the stress appears to have migrated to the spring tunnel. This may be partly induced by the fixtures, however it requires further investigation.

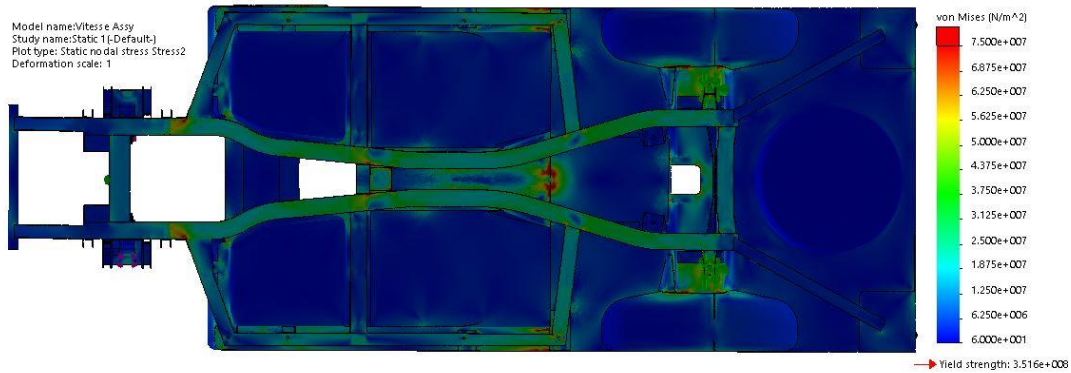


Figure 31: Von Mises Stress plot of the standard Vitesse structure at 1000Nm

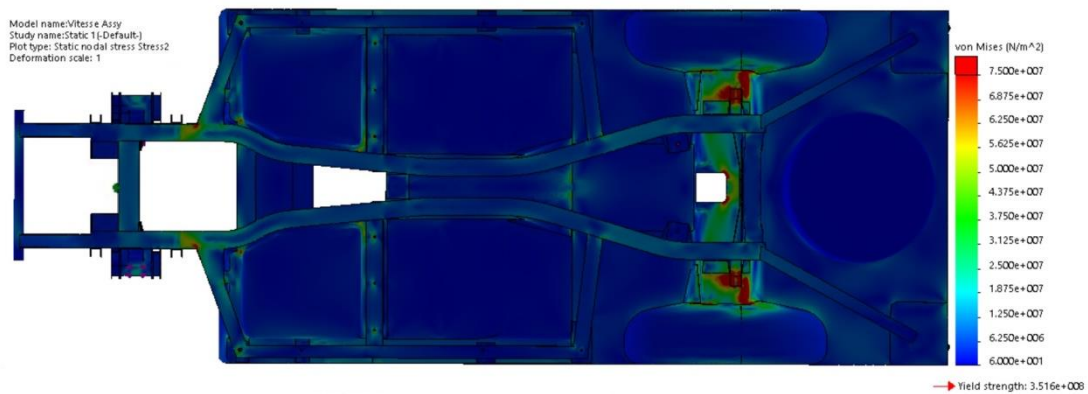


Figure 32: Von Mises Stress plot of the standard Vitesse structure with a pseudo roll cage at 1000Nm - raising torsional rigidity to over 6000Nm

Various modifications were simulated, including those in Tables 15 and 16.

Table 15: Table of chassis modifications and their simulated effect on overall torsional stiffness. See Appendix 18 and 20 for more details.

Configuration	Run #	Overall Stiffness Nm/°	Stiffness Increase %	Weight Increase %
Standard Chassis	36	1116	-	-
Side-Rails	38	1338	1.6	4
Boxed Front Outrigger *	39	1383	19.3	5
Boxed Mid Outrigger *	40	1449	23.0	6
T-Shirt Plate	42	1149	2.9	4
Bolt in Cross-Member	44	1256	11.2	2.7

* Simulation Includes Previous Feature

Table 16: Table of body modifications and their simulated effect on overall torsional stiffness. See Appendix 19 and 20 for more details.

Configuration	Run #	Overall Stiffness Nm/°	Stiffness Increase %	Weight Increase %
Standard Body (No Doors)	1	2573	-	-
Extra Body Mounts	4	2610	1.4	0.33
Integral Rear Crossmember and Basic Sill	6	3596	28.5	2.7
Full Sill	17	3909	35	4.8
H-Frame/ Dashboard Brace*	23	4331	40.6	6.5
Steel Gearbox Tunnel	24	2767	7.1	1.9
Pseudo Roll Cage	28	6641	61	-

* Simulation Includes Previous Feature

For the greatest effect, modifications should be as far as possible from the neutral axis as shown in the parallel axis theorem, therefore a roof or roll cage structure would have the greatest possible effect. However, this is ruled out in the specification so the next best thing is to position a modification at the full width of the vehicle.

Both Herald and Vitesse are originally fitted with cosmetic sill panels of pressed steel fitted with screws, as in Figure 33 (Canley Classics, 2020 & Standard Triumph, 1962). Replacing this panel with a stiff beam either fabricated into the body or as a separate bolt-in structure would increase overall stiffness. This modification would not change the look of the vehicle and is in a perfect location to reduce loading on the doors. In addition, any added weight is kept low and between the wheels. Any design must ensure the added geometry does not act to trap debris and increase the rate of corrosion.

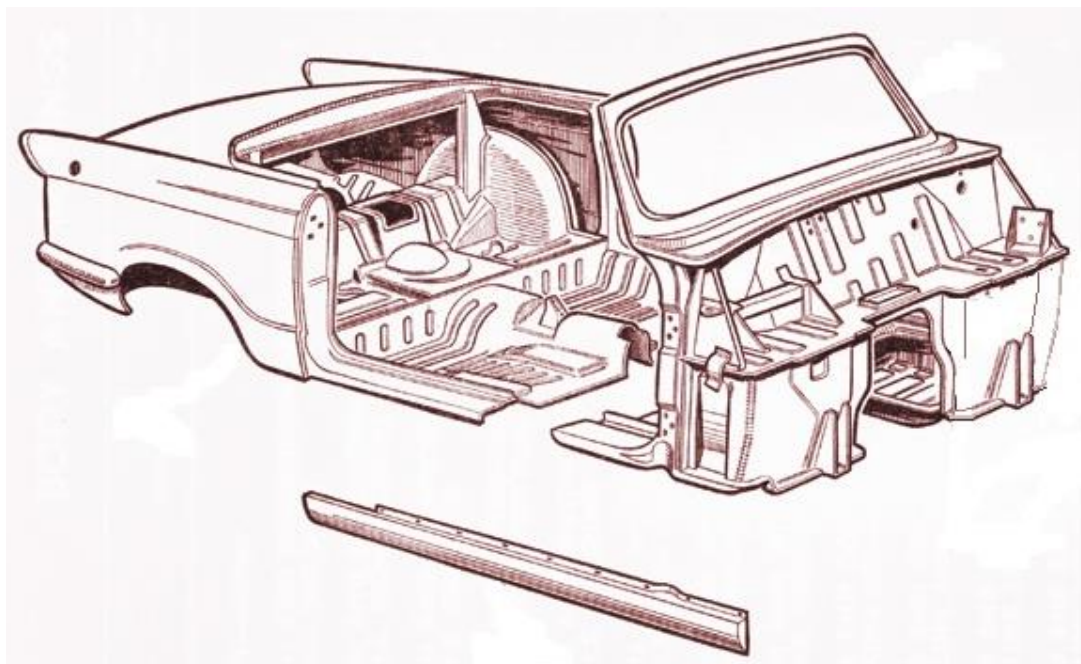


Figure 33: Original cosmetic sill panel, reproduced by kind permission of Canley Classics

The proposed structure was added to the virtual model as in Figure 34, and subjected to an FEA. The results suggest an improvement of 35% or 1350Nm/deg. Combined with the modifications tested above this gives an overall stiffness of 5400Nm/deg, or 4800Nm/deg with the roof down – almost equivalent to the 1998 BMW Z3 with a stiffness of 5600Nm/deg (roof up) (YouWheel, 2016).

The new stiffness of 5400Nm/deg is 7.2x the calculated roll stiffness which is within the target range of 6.8 – 30 as suggested by Dixon (1996), though this drops to 6.5x with the roof down. Roll stiffness calculations are illustrated in Appendix 3.

These results are based on a hollow beam constructed from 1.2mm sheet metal with reinforcing gussets at each body mount. The predicted improvements cannot be considered as reliable as chassis predictions, since body modifications have not been fully verified against real world testing, however this is a sensible ballpark figure based on the evidence obtained.

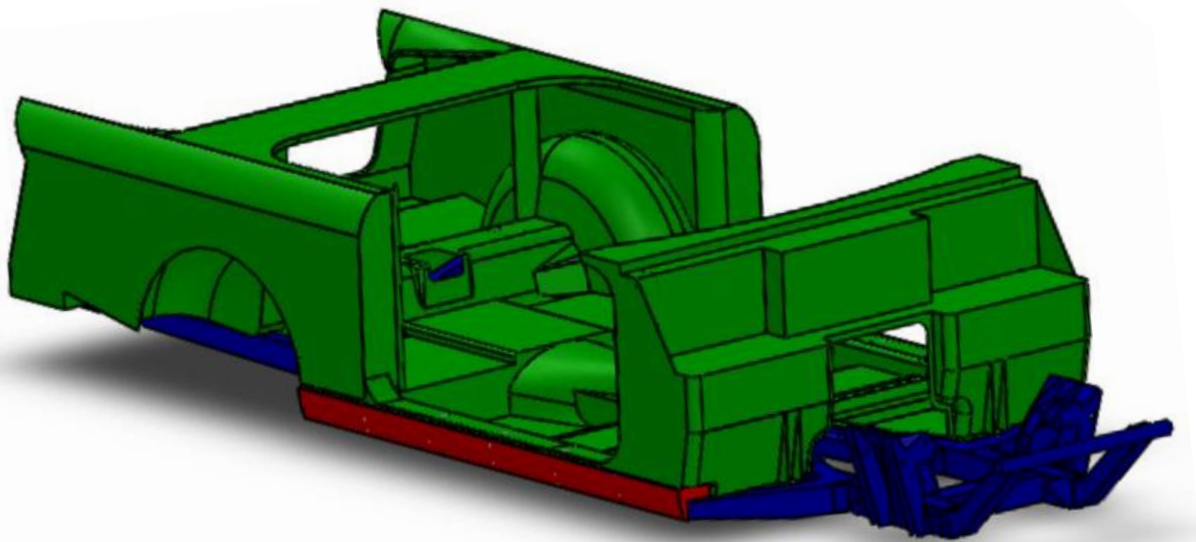


Figure 34: Simulated sill structure, fabricated from 1.2mm steel.

Conclusions

Overall, all project objectives have been addressed and the aims largely met. The vehicle structure was modelled in Solidworks (2017) and the torsional stiffness quantified through FEA. These models have been successfully validated through physical testing, and two modifications have also been tested and virtual models validated. The chassis was found have a stiffness of 1250Nm/deg $\pm 5\%$ with the bolt on body structure increasing stiffness by 90%, and the doors and convertible roof adding a further 20% each bringing the total stiffness to 3500Nm/deg $\pm 12\%$. Chassis stiffness was increased by 37% by boxing the side-rails and adding an additional bolt-in cross-member, thus increasing assembled vehicle stiffness by 13%. The experimental results validated the FEA of the modified model, increasing confidence in the results of further simulated modifications. These results suggest that converting the original cosmetic sill panel into a structural member strongly tied into the vehicle body and chassis, could increase overall vehicle stiffness by 35%. This would mean a torsional stiffness of 5400Nm/deg putting the Vitesse in the same ball park as the BMW Z3 with a stiffness of 5600Nm/deg (YouWheel, 2016).

Recommendations

Future studies would benefit from the use of technology; remote sensors bonded to the chassis would eliminate human error from twist measurements and could measure more data points, faster and with greater precision. It may also be useful to direct measurement to the weak areas highlighted to generate better resolution in these key areas.

It would be interesting to repeat the experiment on a saloon or estate variant, or a convertible of different age to determine if differences in manufacture or mileage make a measureable difference. Furthermore, the Triumph GT6, built on a very similar backbone chassis, would be highly comparable, thus highlighting the effectiveness of a semi-monocoque body structure. These effects could also be approximated using the Stressed Structural Surfaces method, discussed in appendix A.

An area largely neglected in this study is the chassis/body interface. It may be possible to simulate this as an assembly in Solidworks, and determine if there is a significant difference.

Acknowledgements

Adam Kyte – For keeping me on track.

Nick Jones – For offering advice and enthusiasm, and the use of car and workshop.

Duncan Palmer – For the loan of his tractor weights.

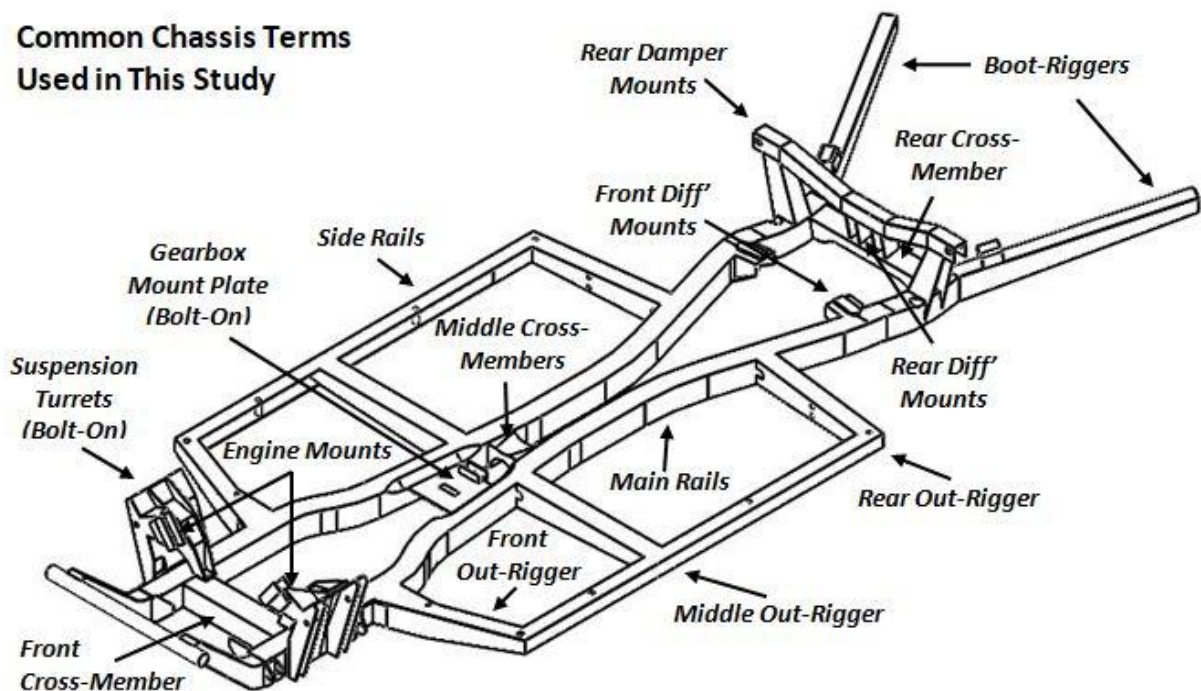
P.J. Pettifor – For his detailed study of the Triumph Spitfire.

Nomenclature

AISI – American Iron and Steel Institute
 A_m – Area enclosed by median line (m^2)
 BL – British Leyland
 CAD – Computer Aided Design
 Diff – Differential
 DOF – Degrees of Freedom
 E – Youngs Modulus (GPa)
 FBD – Free Body Diagram
 FEA – Finite Element Analysis
 FMECA – Failure Mode Effect & Criticality Analysis
 G – Shear Modulus (MPa)
 I_z – Second Moment of Area

J – Torsional Constant (m^4)
 K – Shape Constant (m^4)
 K_δ – Bending Stiffness
 K_θ – Torsional Stiffness
 K_θ – Torsional Stiffness (Nm/Degree)
 L – Length
 LH – Left Hand
 I_m – Median Line (m)
 MIG – Metal Inert Gas
 RH – Right Hand
 T – Torque (Nm)
 δ – Deflection (mm)
 ρ – Density (kg/m^3)
 σ – Bending Stress (MPa)
 τ – Shear Stress (MPa)

Common Chassis Terms Used in This Study



References

- ASM International (2008) *Elements of Metallurgy and Engineering Alloys – Chapter 14 Fatigue*. Available at: https://www.asminternational.org/documents/10192/1849770/05224G_Chapter14.pdf (Accessed: 10/03/2020)
- Autocar (1962) 'Triumph Vitesse', *Autocar* (May)
- Alvi, M.S.I. (1978) *The stress distribution in the joints of vehicle chassis frames subject to torsion*. PhD Thesis. Cranfield Institute of Technology School of Automotive Studies. Available at: <http://hdl.handle.net/1826/3629> (Accessed: 03/12/19)
- Automobile Engineer (1965) *Austin 1800, Automobile engineer*. Available at: <http://copeland.id.au/wp-content/uploads/2010/05/Austin-1800.pdf> (Accessed: 28/11/19)
- Bensted-Smith, R. (1960) *TURN LEFT FOR TANGIER: The Hard Way for Heralds*. Coventry: Standard-Triumph Organisation.
- Bhote, K. (2005) *History of Standards in India*. Available at: www.standardmotorclub.org.uk/cars/india/standardindia.htm (Accessed: 03/12/19)
- Braess, H. and Seiffert, U. (2005) *Handbook of Automotive Engineering*. USA: Society of Automotive Engineers.
- Canley Classics (2020) Triumph Vitesse. Available at: www.canleyclassics.com/triumph-vitesse/ (Accessed: 03/12/2019)
- Clarke, RM. (1998) *Triumph Vitesse 1962 – 1971*. Wisconsin: Motorbooks international.
- Club Triumph Forum (2015) 'Reinforced Vitesse Chassis' Thread started 11/02/15 by 'oil_on_the_carpet' Available at: club.triumph.org.uk/menu/6134/item/124324/view?messagepage=1 (Accessed: 03/12/2019)
- Davies, G. (2012) *Design and material utilization. Materials for Automobile Bodies*. 2nd edn. USA: Butterworth-Heinemann.
- Davies, J (2016) *The Lightweight Cars Competitors And Their Structures*. Available at: www.ukessays.com/essays/engineering/the-lightweight-cars-competitors-and-their-structures-engineering-essay.php (Accessed: 03/12/2019)
- Deakin. A, Crolla. D, Ramirez. JP and Hanley. R, (2000) 'The Effect of Chassis Stiffness on Race Car Handling Balance', *Proceedings of the 2000 SAE Motorsports Engineering Conference & Exposition*, pp.361.
- Dixon, J.C. (1996) *Tires, Suspension and Handling*. 2nd edn. USA: Society of Automotive Engineers.
- Geithner, P. (2013) *Triumph Spitfire & GT6 Spring Rates and resultant Wheel Rates and Roll Stiffnesses*. Available at: http://auskellian.com/paul/links_files/springs.htm (Accessed: 29/11/2019)

Government of South Australia (2019) *Torsional rigidity and beaming stiffness test procedures MR810*. Available at:

www.sa.gov.au/data/assets/pdf_file/0004/8752/MR810-Torsional-rigidity-and-beaming-stiffness-test-procedure-8.14.pdf (Accessed: 03/12/2019)

Haynes, JH. (1973) *Triumph Vitesse and GT6, Owners Workshop Manual*. Yeovil: Odcombe Press.

Hibbeler, RC. (2011) *Mechanics of Materials*. 8th edn. Boston: Prentice Hall.

Karayan. A, Castaneda. H, Ferdian. D, Harjanto. S, Nurjaya. D, Ashari. A (2012) *Finite Element Analysis Applications in Failure Analysis: Case Studies*. Available at: https://www.researchgate.net/publication/263848132_Finite_Element_Analysis_Applications_in_Failure_Analysis_Case_Studies (Accessed: 10/04/2020)

Markus, F. (2012) *2012 Tesla Model S First Drive, Motor Trend*. Available at: www.motortrend.com/news/2012-tesla-model-s-first-drive/ (Accessed: 28/11/2019)

Milliken, W.F. and Milliken, D.L. (1995) *Race Car Vehicle Dynamics*. USA: Society of Automotive Engineers.

Nisbett, KJ. and Budynas, RG. (2015) *Shigleys Mechanical Engineering Design*. 10th edn. McGraw-Hill Education.

Parkers (No Date). *Porsche 911 Cabriolet (1998-2005) Specs & Dimensions*. Available at: [www.parkers.co.uk/porsche/911/cabriolet-1998/911-\(996\)-turbo-s-2d/specs/](http://www.parkers.co.uk/porsche/911/cabriolet-1998/911-(996)-turbo-s-2d/specs/) (Accessed: 10/02/20)

Pettifor, PJ. (1991) *Enhancing the Torsional Stiffness of the Triumph Spitfire*. Shrivenham: Royal Military College of Science.

Poynting, JH. (1909) 'The wave motion of a revolving shaft, and a suggestion as to the angular momentum in a beam of circularly polarised light', *The Royal Socieity*, 82(557). doi: 10.1098/rspa.1909.0060

Prelims, R. (2010) *Automotive Chassis Design*. Available at: http://web.iitd.ac.in/~achawla/public_html/736/3-Automotive_chassis-design-v2.pdf (Accessed: 03/12/2019)

Robertson, J. (2002) 'Chassis Design and Analysis', in Happian-Smith, J. (ed.) *Introduction to Modern Vehicle Design*. Oxford: Butterworth-Heinemann, pp.125-155.

Roots, M., Brown, J., Anderson, N., Wanke, T., Gadola, M. (1996) 'The Contribution of Passenger Safety Measures to the Structural Performance in Sports Racing Cars,' Cranfield: Cranfield University.

Sideways Forum (2019) 'Chassis Stiffening' Thread started 01/09/19 by 'NeilR' Available at: <http://sideways-technologies.co.uk/forums/index.php?topic/8187-chassis-stiffening/> (Accessed: 03/12/2019)

Solidworks (2013) Mesh property manager. Available at: https://help.solidworks.com/2018/English/SolidWorks/cworks/IDC_HELP_MESH_SOL_ID.htm (Accessed: 10/01/2020)

Solidworks (2017) *Meshing*. Available at:
www.help.solidworks.com/2017/English/SolidWorks/cworks/c_shell_mesh_top.htm
(Accessed: 03/12/19)

Standard Triumph (1962) *Body Herald Range Vitesse Service Training Notes*.
Available at: <http://vitessesteve.co.uk/ServiceTrainingNotes> (Accessed: 20/11/2019)

Staniforth, A. (1997) *Race and Rally Car Source Book: The Guide to Building or Modifying a Competition Car*. 4thedn. Edinburgh: T.N.Foulis.

Thomason, J. (2003) 'Twisted!', *Courier*, 273a, pp.54-61.

Velie, H.D. (2016) *Chassis Torsional Rigidity Analysis for a Formula SAE Racecar*.
Available at: <https://deptapps.engin.umich.edu/open/rise/Chassis+Torsional+Rigidity+Analysis+for+a+Formula+SAE+Racecar.pdf> (Accessed: 03/12/2019)

Webb, G.G. (1984) *Torsional stiffness of passenger cars*. London: Institute of Mechanical Engineering.

Young, WC., Budynas, RG. (2002) *Roarks formulas for stress and strain*. 7th edn. McGraw-Hill.

YouWheel (2016) *Car Body Torsional Rigidity: A Comprehensive List*. Available at:
<http://youwheel.com/home/2016/06/20/car-body-torsional-rigidity-a-comprehensive-list/> (Accessed: 03/12/19)

Appendices are provided as 'supplementary files' (see download area).